

High-power picosecond electronics

G A Mesyats, M I Yalandin

DOI: 10.1070/PU2005v048n03ABEH002113

Contents

1. Introduction	211
2. Picosecond switching processes	212
3. Energy storage	214
4. Schematic of picosecond generators	215
5. Pulse-periodic picosecond generators	218
6. Employment of high-power picosecond pulses	219
6.1 Picosecond electron diodes; 6.2 Picosecond X-ray sources; 6.3 Formation of magneto-insulated electron bunches;	
6.4 Generation of high-power picosecond microwave pulses; 6.5 Sources of super-broadband radio-frequency radiation	
7. Conclusion	227
References	228

Abstract. This paper reviews current research in high-power picosecond electronics, a branch of experimental engineering physics, whose dynamic development critically depends on national priority research projects. The aim of the review is basically to show progress in the study of picosecond processes involved in the accumulation, commutation, and transformation of high-density electric power. Examples are presented demonstrating what the latest built high-voltage picosecond facilities will potentially fundamentally contribute to developments in generating unique-property high-power electron beams and electromagnetic radiation pulses.

1. Introduction

The general aim of pulse power engineering and electronics is to master a high power of voltage sources, particle bunches, and electromagnetic radiation. This objective is accomplished by increasing the energy transferred by a pulse generator to an appropriate load. At a fixed energy store, the power can be increased by reducing the time of energy release (energy compression), i.e., by shortening the pulse duration.

The problems that stimulated the creation of high-power pulse generators are historically of both research and

practical character. These are extreme tests of insulating strength for conventional energy systems (lightning guard), radiography of fast processes (implosion, ballistics), non-destructive flaw detection, the physics of exploding conductors and detonation processes, fusion plasma heating, long-distance radars, nuclear-physical experiments, etc.

Investigations and developments concerning the trends mentioned resulted in consistently mastering the range of durations 10^{-8} – 10^{-9} s in the 1970s. Then, high-voltage nanosecond generators were created with a storage energy of dozens of megajoules, a voltage up to 10^6 – 10^7 V, a current greater than 10^6 A, and pulsed power exceeding 10^{12} W. In this way, a new physical and technical field of activity was formed, namely, high-power nanosecond power engineering and electronics [1, 2]. Certain objective factors played a great role in this process.

Generally, these investigations were in demand and were sufficiently provided with resources, although the corresponding results were not an alternative to conventional electrical power engineering. In scientific and technical aspects, the investigations were based on progress in studying fast switches, the development of power semiconductor electronics, the creation of insulating materials with high electric strength, and the study of gas discharges and vacuum emission.

In addition, it was important to continuously update the element basis of devices and to develop metrological units, methods of mathematical modeling, and calculation for high-voltage systems. We may also recall a kind of ‘feedback’, i.e., an influence of the requests of developing high-power high-voltage nanosecond equipment on the progress in the scientific industry, the science of materials, and other fields mentioned.

The next stage in the development of high-power high-voltage systems might seem to come as naturally as the transfer from the microsecond to the nanosecond duration range. However, considerable difficulties in transferring to the picosecond range were encountered, which prevented one

G A Mesyats P N Lebedev Physics Institute,
Russian Academy of Sciences,
Leninskii prosp. 53, 119991 Moscow, Russian Federation
Tel. (7-095) 135 24 30. Fax (7-095) 952 50 81
E-mail: mesyats@pran.ru

M I Yalandin Institute of Electrophysics,
Ural Branch of the Russian Academy of Sciences,
ul. Amundsena 106, 620016 Ekaterinburg, Russian Federation
Tel. (7-343) 267 87 85. Fax (7-343) 267 87 94
E-mail: yalandin@iep.uran.ru

Received 15 November 2004

Uspekhi Fizicheskikh Nauk 175 (3) 225–246 (2005)

Translated by N A Raspopov; edited by A M Semikhatov

from speaking about high-power picosecond electronics for a long time. The mere imperfection of detecting devices hindered the study of processes with a duration much shorter than 10^{-9} s, and the level of metrological support is still the determining limiting factor in the picosecond range.

We can understand the complexity of the problem if we recall that the dynamics of energy acquisition, switching, and transformation in a characteristic time scale of 10^{-10} s implies real-time detection of the processes that are comparable in duration with the period of high-frequency oscillations of UHF generators operating in the 10 GHz range conventionally used in radar technology. The corresponding spatial scale of formative picosecond circuits does not exceed a few centimeters at typical potentials near hundreds of thousands volts.

Electro-physical processes of picosecond duration are sufficiently frequent in experimental practice. But they remained out of the picture until special broadband oscilloscopes and detecting sensors with a corresponding temporal resolution were developed. The boundary between nanosecond and picosecond devices was, consequently, conditional. Among pulsed devices developed during the last few decades, there were numerous experimental installations capable of generating high-power picosecond pulses. Publications concerning such investigations and aimed at generating nanosecond pulses with the pulse rise time shorter than 10^{-9} s can be traced back more than fifty years (see, e.g., [3]). Pulsed voltage generators with such characteristics should be classified as picosecond devices.

The necessity of obtaining high-power voltage pulses with the total duration shorter than one nanosecond is determined by specific demands arising in investigations of fast electric-discharge and emission processes with the temporal resolution 10^{-10} – 10^{-11} s [4–6] and the generation of short-duration high-power X-ray pulses [7], electron bunches [8, 9], and super-broadband radio pulses [10, 11]. These problems effectively stimulated the development of high-power picosecond electronics based on formation, transfer, and measurement of pulses with a duration shorter than 1 ns at the voltage up to 1 MV.

Similarly to the devices in the nanosecond range, high-power picosecond systems are based on voltage pulse generators with a corresponding pulse duration. Small dimensions and consumed power make them promising devices for obtaining a high density of power at relatively low expenses. Nevertheless, the picosecond-duration range has certain specific features. The approach to the development of a generator is still a sequential compression (namely, time-amplitude compression) of energy.

Hence, a picosecond generator can be presented as a chain of energy compressing devices, each of them including a charge (transmitting or transforming) unit, an energy storage unit, a switching unit, and a load. A nanosecond compression unit almost always precedes a picosecond unit. This is the result of the obvious contradiction between the required high electrical strength of the energy storage unit (usually a storage capacitor) and the short response time of switch operation. The picosecond duration of switching is usually provided by a high overvoltage level in the switch [12], which can be realized at a sufficiently short time of high potential action such that the breakdown effects in the energy storage unit are ‘delayed’.

Development of high-power picosecond electronics required the creation of compact electrically strong energy storage, high-voltage fast switches, broadband transmission

lines, and detecting devices. Presently, wide experience in constructing nanosecond generators of various powers makes it possible to impose the requirements that are specific for the picosecond range and to determine basic techniques for calculating and constructing such devices. In this review, we focus our attention on the investigations of physical processes occurring in various switches, formative methods for high-power picosecond pulses, and the corresponding applications in various fields: electrophysics, emission electronics, accelerating technique, relativistic UHF electronics, etc.

2. Picosecond switching processes

The general requirement imposed on the discharge switching units in the picosecond range is a switch transfer from a non-conducting state to a high-conducting state in a switching time shorter than $t_s \ll 1$ ns. Generally, a switch consists of two metal electrodes separated by a medium possessing an abrupt dependence of the current on the voltage applied. A solid dielectric, liquid, gas, or semiconductor structure can be chosen as such a medium.

The last two decades have been marked by a certain success in the development of fast semiconductor switches [13]. At the same time, gas spark switches are still the most commonly used devices in high-power picosecond electronics, where the time of switching the power from hundreds of megawatts to a few gigawatts is of the order 10^{-10} s. Some advantages of gas switches are the possibility of adjusting their parameters and simple manufacturing and operation. In addition, gas discharge is well studied in the range $t_s \ll 1$ ns [4].

A short switching time is achieved by using high pressure in a spark gap or high overvoltage applied across the gap [1, 14]. If the conditions of the discharge are close to static, then the switching time can be found from the Rompe–Weitzel model [1],

$$pt_s \approx \frac{K_r(p/E)^2}{a}, \quad (1)$$

where p is the gas pressure, E is the electric field strength at which the discharge occurs, K_r is the coefficient dependent on the front duration for the voltage pulse across the gap (usually, $K_r \approx 10$ – 20 [1]), and a is a gas-specific constant (for air and nitrogen, $a = 0.8$ – 1 atm cm² s⁻² V⁻²).

If the discharge occurs at a constant voltage, then, according to the Paschen law, the ratio $E/p = \text{const}$, and hence $t_s \propto p^{-1}$. It follows from expression (1) that for obtaining $t_s < 1$ ns, the required pressure must be $p > 10$ atm, and at $t_s = 100$ ps, the pressure of air or nitrogen must be $p = 100$ atm. Unfortunately, the current cannot exceed 1–10 kA under these conditions due to the inductance of the arising spark channel, which considerably limits the rate of current rise.

At a large current through the gap, a shorter switching time can be obtained by applying a considerable overvoltage across the gap using a large number of initiation electrons, which results in a volume mode of gas discharge [1]. If the gap capacitance and discharge circuit resistance are neglected, we have

$$t_s = (\alpha v_e)^{-1} \ln \frac{I_0 d}{e N_0 v_e}, \quad (2)$$

where α is the impact ionization factor, v_e is the electron drift velocity in the gas, I_0 is the current corresponding to the

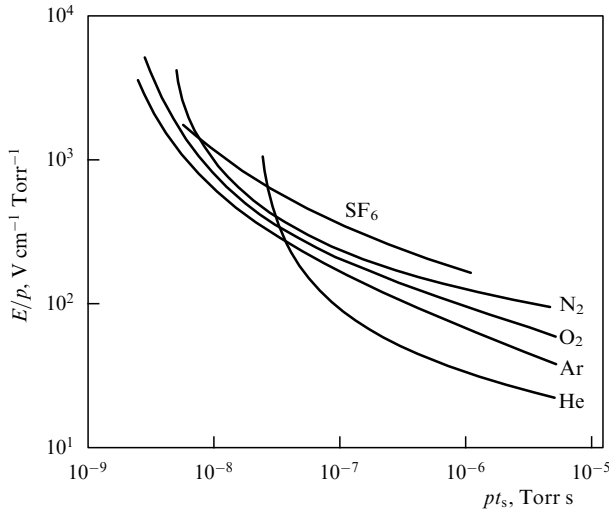


Figure 1. Similarity law for the breakdown formative time in various gases [15].

instant from which time t_s is counted (usually, I_0 corresponds to 10% of the current amplitude), d is the gap length, e is the electron charge, and N_0 is the number of initiating electrons.

The dependence $pt_s = f(E/p)$ for various gases [15] is shown in Fig. 1. One can see that at $p = \text{const}$ with an increase in E , due to the quick rise of α and v_e , the switching time reduces and reaches $t_s < 1$ ns even at atmospheric pressure of nitrogen in the case where $E > 10^5$ V cm $^{-1}$. This value exceeds the static breakdown field strength for air by a factor of three at atmospheric pressure. A specific feature of pulsed discharge at a large value of E and high gas pressure and a current is the absence of a contracted channel. It is obvious that the reduced inductance of such a discharge gap makes switches of this type preferable for the picosecond range.

At moderate voltages, generation of high-current picosecond pulses is usually realized by discharging a low-inductance capacitor through an avalanche gas switch [1]. The maximum current I_{max} is obtained in the case where the resistance R and inductance L of the circuit are negligible, i.e., $L/R \ll t_s$. In this case, the maximum current is

$$I_{\text{max}} = \alpha v_e U_0 C F(E/p) \quad (3)$$

at the pulse duration

$$t_p \approx [\alpha v_e F(E/p)]^{-1}, \quad (4)$$

where U_0 is the switch puncture potential, C is the capacitance of storage capacitor, and $F(E/p)$ is a function of the ratio E/p .

Taking the resistance R into account results in the function $F(E/p)$ slightly varying, as seen in Fig. 2. From Eqns (3) and (4), it follows that for air discharge at atmospheric pressure, at $E = 10^5$ V cm $^{-1}$ and $C = 100$ pF, the parameters I_{max} and t_s are 1 kA and 0.1 ns, respectively. Close values were obtained in experiments at two-fold and greater overvoltage across the spark gap [1].

A picosecond switching time can also be obtained in discharge switches at a gas pressure lower than atmospheric pressure. The spark discharge that operated on the left branch of the Paschen curve was tested in [16]. The parameters of pulses were close to those obtained with high-pressure switches.

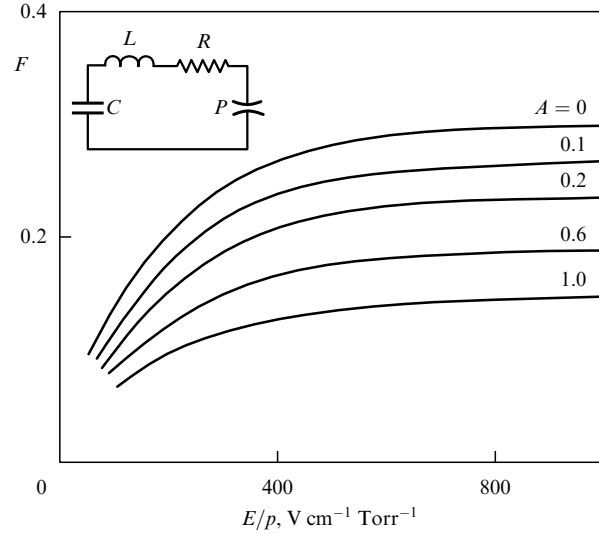


Figure 2. The function $F(E/p)$ at various values of $A = \alpha v_e RC$ and $L = 0$.

There are other types of switches suitable for certain applications in the picosecond range, e.g., mercury switches [17] capable of forming pulses with the rise time 0.1 ns at voltages up to 1 kV, switches with a discharge along the surface of the dielectric in a vacuum [1], and a large number of short (about 0.1 mm) gas gaps connected in series, which operate without adjustment in a wide range of voltages [18].

Switches employing the breakdown of liquid and solid dielectrics are rarely used because they are complicated, unstable, and rather difficult to operate because of the necessity of changing the dielectric after each pulse. For example, a ruby laser with a power of 20 MW was used in order to obtain the switching time $t_s = 50$ ps for a solid switch [19]. On the other hand, a simple high-pressure gas spark switch triggered a voltage of 30 kV in the time lapse 0.12 ns by a laser with the power 1 MW [20].

Magnetic switches and lines with impact electromagnetic waves also operate in the picosecond range. In particular, as was mentioned in [2], the front duration of a stationary blast electromagnetic wave in a long-distance ferrite-filled line is $t_r \approx k/\gamma H$, where γ is the gyromagnetic ratio for electrons, H is the magnetic field strength in the line at the peak current, and k is the coefficient of the order of a few units determined by the initial and saturated ferrite magnetization. In order to obtain $t_r \sim 10^{-10}$ s, the parameter H must be of the order of a few kOe.

As far as modern semiconductor switches with fast rise times of voltage and current [13] pulses are concerned, the physical processes in such systems require a particular consideration. We note that the delay in the breakdown of the $(p-n)$ -junction followed by the formation of an impact-ionization wave in the silicon diode based on the single semiconductor structure makes it possible to switch to a power of a few hundred kW in the picosecond range. It is clear that a separate semiconductor structure has a limitation in the switching voltage at the level of a few kV.

The formation of pulses with a power of dozens or hundreds of MW and higher can be realized by a series-parallel connection of high-voltage assemblies of semiconductor structures (see Fig. 3a). In [21], the experimental results are presented on using semiconductor diode sharpeners with a delayed impact-ionization wave for forming

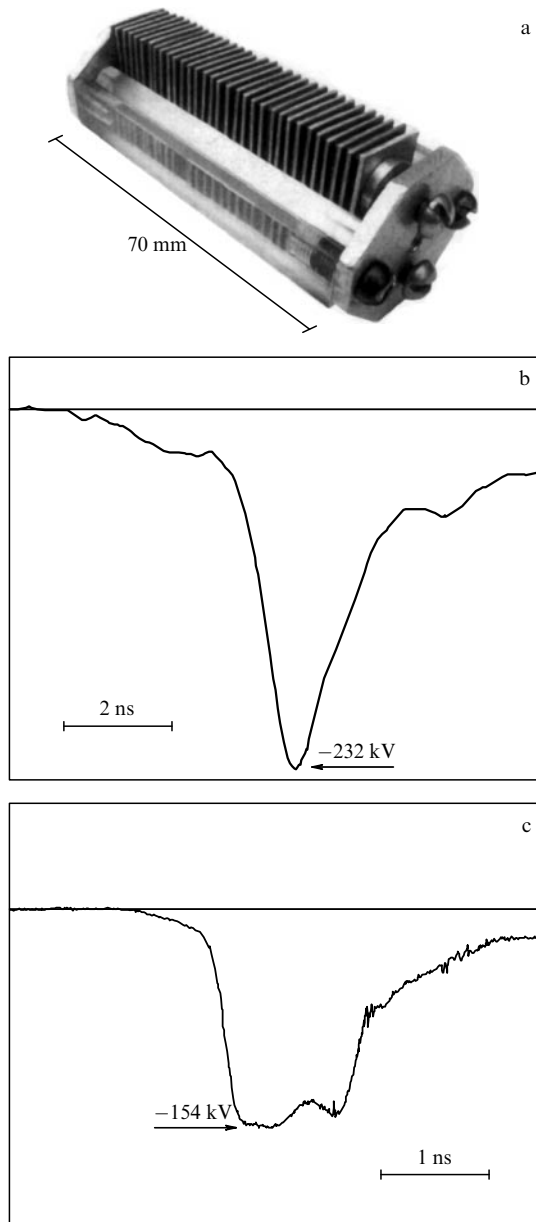


Figure 3. (a) A semiconductor diode sharpener formed by two parallel sections each comprising 120 silicon structures connected in series, which provide formation of the pulse (b) with the front duration 1 ns. (c) Oscillogram of the voltage pulse with the front duration 200 ps obtained by means of a semiconductor diode sharpener with a tunneling-impact formation mechanism of ionization front. The pulsed switched power is 500 MW [21, 22].

high-voltage pulses with a duration of 1–2 ns on a 50-Ω load. The corresponding pulse power was 0.75–1 GW at the repetition frequency up to 3.5 kHz. At the voltage 230 kV, the switching time was close to 1 ns (see Fig. 3b) and the maximum voltage rate on the load was $dU_r/dt \approx 1.9 \times 10^{14} \text{ V s}^{-1}$. Under these conditions, the diode assemblage (three parallel sections, each comprising 144 structures connected in series) had considerable parasitic parameters, which hindered the detected pulse rise time.

In [22], an even faster switching of a dense current ($dI/dt \geq 10 \text{ kA ns}^{-1}$) was realized in diode structures due to the formation of the tunneling-assisted impact ionization front considered theoretically in [23, 24]. In this case, a

voltage drop with the ramp $dU_r/dt \approx 1.9 \times 10^{14} \text{ V s}^{-1}$ passed from the previous cascade to an assemblage comprising 20 structures connected in series. In this way, pulses were obtained with the total duration 1 ns and rise time 200–250 ps at the voltage amplitude 150–160 kV and pulsed power up to 500 MW (see Fig. 3c).

3. Energy storage

In addition to fast picosecond switches, the most important elements included in formation schemes of high-power pulses are energy storages. The voltage amplitude of 10^5 – 10^6 V is obtained by using the compact capacitive storages that are usually presented by strip, disk, or, mostly, coaxial capacitors (lines). Their output energy is determined by insulation strength, i.e., the possibility to withstand the overvoltage that activates a nearby picosecond switch. Hence, an enhancement of the energy capacity and an increase in the picosecond generator power are close problems, which, however, impose conditions that are opposite to fast switching.

In coaxial energy storages, transformer oil or high-pressure gas is conventionally used as a dielectric medium. As was shown [25], the electric field intensity at which transformer oil breaks down increases by a factor of ten if the duration of voltage action changes from 100 ns to 100 ps. At the duration $t_p \approx 1 \text{ ns}$, the electric field intensity is $E_{\text{max}} \approx 5 \times 10^6 \text{ V cm}^{-1}$, and at $t_p \approx 200 \text{ ps}$, the value of E_{max} exceeds 10^7 V cm^{-1} .

The electrical strength of a gas insulator under the conditions of static breakdown is determined by the Paschen law. Conventionally, the far branch of the Paschen curve is used in a picosecond technique. The electric strength of insulation depends on a particular gas, the preferable one being sulfur hexafluoride (SF_6) or its mixture with nitrogen. Nitrogen at the pressure up to 100 bar or hydrogen are the gases most frequently used for insulating purposes. Hydrogen is preferable at high repetition frequencies.

It is known that the rate of pulse rise in switching the energy storage with a coaxial line may be limited due to the excitation of higher modes with a frequency dispersion if there are nonuniformities in the tract [26, 27]. The minimum pulse rise time is determined by the excitation boundary for the transverse electric wave of the TE-type at the lowest critical frequency. At a fixed diameter D_2 of the external conductor of the coaxial line, the minimum electric field strength on the internal conductor of diameter D_1 is obtained in the case where $\ln(D_2/D_1) \approx 1$. We can estimate the shortest pulse rise time t_r that is obtained in the limit of the breakdown strength of storage insulation. This minimum front duration and the duration of the picosecond pulse itself that is close to this value are determined by the relation

$$t_r \approx 1.5 \times 10^{-10} \sqrt{\varepsilon} \frac{U_a}{E_{\text{max}}}, \quad (5)$$

where E_{max} is the maximum admissible electric field strength on the internal conductor expressed in V cm^{-1} and U_a is the voltage amplitude (in volts).

Relation (5) implies that at megavolt voltages, the pulse front duration $t_r = 10^{-10} \text{ s}$ is obtained at a sufficiently high electric field strength of 10^7 V cm^{-1} and a small permittivity of the ambient medium $\varepsilon < 2$. Insulation provided by a high-pressure gas is preferable ($\varepsilon = 1$).

Actually, it is not only the insulation properties of the line that limit the pulse front duration from ‘below’, but to a

higher degree it is determined by other factors, such as a switch triggering delay or nonuniformities of the transmitting channel, due to which the pulses spread and their amplitude falls [17]. A ‘perfect’ switch, however, cannot allow obtaining the parameters predicted by expression (5) in real high-voltage constructions, because the voltage should be lowered below the breakdown threshold for storage unit insulation.

Indeed, even if a gas medium is integrated with a spark switch, a picosecond compression section should be separated from the previous cascade and output channel by the massive bushing insulators capable of withstanding high pressure. Usually, the insulator permittivity is $\epsilon > 3$, which noticeably distorts the electric field inside the coaxial line. Moreover, the electric strength of the whole unit may be weakened by the possible breakdown of the insulator surface, the discharge initiation at the triple point metal–dielectric–gas, etc.

4. Schematic of picosecond generators

There are several schemes used for generating picosecond pulses. The simplest one is a direct discharge of energy storage, i.e., of a capacitor to a load through a high-pressure switch with the switching time $t_s \ll 1$ ns. If the relation

$$t_s \ll \frac{l\sqrt{\epsilon}}{c} \quad (6)$$

holds, where l is the characteristic length of the capacitor plate and c is the speed of light, then the limiting pulse duration t_p is determined by the formula

$$t_p = \frac{2l\sqrt{\epsilon}}{c} \quad (7)$$

If inequality (6) holds, the capacitor discharges in the mode of a line with distributed parameters.

In Fig. 4, two schematic diagrams of pulsed current generators with a disk storage capacitor (line) are presented [28]. The pulse duration is determined by the geometry of storage plates and permittivity of ceramic insulators. To

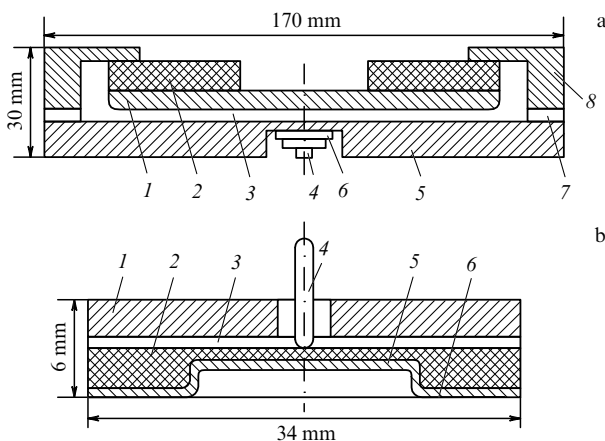


Figure 4. Picosecond current generators [1, 28]: (a) 1, 5 — electrodes; 2 — the dielectric of the capacitor ($C = 6.2 \times 10^{-9}$ F, $\epsilon = 700$); 3 — air gap ($\delta = 3$ mm, $p = 110$ Torr); 4 — initiating electrode; 6 — titanate ceramics for initiating a discharge; 7 — shunt; 8 — case; (b) 1 — electrode; 2 — capacitor ($C = 1.5 \times 10^{-10}$ F, $\epsilon = 80$); 3 — gap ($\epsilon = 0.3$ mm, $p = 760$ Torr); 4 — initiating electrode; 5 — dielectric ceramics layer on the surface of the electrode; 6 — capacitor plate.

avoid the spread of t_s due to contracted spark channels at insufficient overvoltage across the gap, one or both of the switching electrodes are covered by a dielectric layer with a capacitance $C_D \gg C$ [1]. In this case, the appearance of one or several discharge channels does not result in a high conductivity of the gap because the displacement current through the dielectric is small.

In addition, the channels emit photons, which produce, due to the cathode photoeffect, a required number of initiating electrons, whereas an avalanche discharge necessitates at least one free electron. The initial electrons are specially produced at the cathode by illuminating it with ultraviolet radiation from an initiating discharge over a ceramic surface near the anode. Visual observations show that the whole gap volume glows in the case of avalanche switching and there are no separate channels in the discharge. The generator shown in Fig. 4a produces pulses with the duration 5 ns, the current amplitude 60 kA, and the pulse rise time less than 1 ns. The respective values for Fig. 4b are 3 kA and 0.2 ns.

A voltage pulse with the total duration shorter than 1 ns is generated without additional switches if the starting generator forms a jump nanosecond pulse of a picosecond front duration. For example, picosecond quasi-rectangular pulses can be formed on a load with a starting two-channel nanosecond generator and two parallel transmitting lines, through which two voltage jumps of equal amplitudes and opposite sign are transmitted (see Fig. 5a). Another variant is based on the transmitting line with the shorted segment connected in parallel (see Fig. 5b).

In the case corresponding to Fig. 5a, the pulse duration and polarity on the load R_L depend on which of two pulses comes first to the load and how much sooner it occurs. The pulse duration formed by the scheme shown in Fig. 5b is determined by twice the time needed for the wave to pass the shorted segment L_2 . This time can be adjusted by varying the length of the segment. The afterpulses on the load (see Fig. 5b) can be obviated by an appropriate choice of the impedances

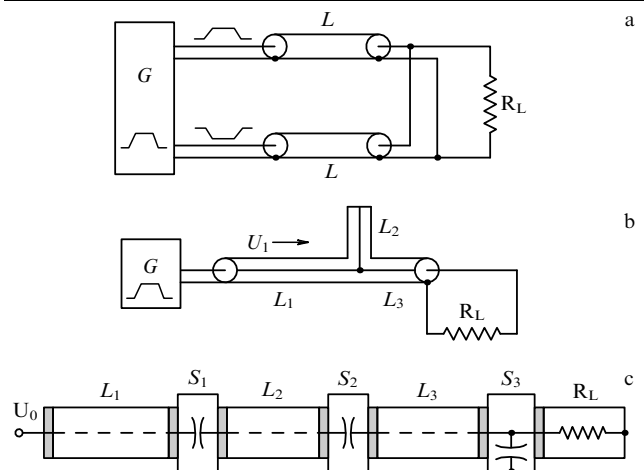


Figure 5. (a) Picosecond generator with two transmitting lines: G — generator of the initial pulse; L — transmitting lines. (b) Generator with shortened formative line: G — generator of initial pulse; L_1 and L_3 — transmitting lines; L_2 — shortened section of the long line; U_1 — wave transmitted from the generator. (c) General schematic of a picosecond pulsed generator: L_1 — nanosecond formative line; L_2 and L_3 — transmitting lines; S_1 , S_2 , and S_3 — nanosecond, picosecond sharpening, and chopping spark gaps.

of the lines, such that the inverted-polarity wave reflected from the shorted end of line L_2 compensates the wave in line L_3 . However, if the impedances of lines L_1 and L_3 in such a scheme are equal, then the output pulse amplitude is twice as low as the initial voltage jump and additional pulses reflected from the beginning of line L_1 arise.

Devices with a shortened line of variable length (see Fig. 5b) are of particular interest for converting a unipolar pulse to a bipolar one. Picosecond pulses with a shape similar to a single-period sinusoid have significant applications in radio systems [10, 11]. The duration of the pulse to be converted must be twice as long as the delay in line L_2 .

In order to obtain symmetric bipolar blades of the pulse, the impedances of lines L_1 and L_3 should be equal and that of line L_2 must be two times lower. In this case, the total amplitude excursion (jump) in line L_3 is equal to the amplitude of the converted unipolar pulse and the energy of the bipolar pulse is 50% of the initial value. Because the absolute value of the amplitude of each opposite blade is two times lower than that of the initial pulse, this positively influences the electrical strength of systems in which the maximum amplitude jump is important.

A passive bipolar converter with a shortened line has an obvious advantage in the stability of the output pulse shape, which is entirely determined by the characteristics of the generator of the initial unipolar pulses. One more advantage is the possibility of smoothly adjusting the pulse duration by varying the electrical length of shortened line L_2 in accordance with the duration of the initial unipolar pulse.

All the picosecond generators of unipolar pulses based on short forming lines and gas spark discharges mainly operate according to the general scheme shown in Fig. 5c. Subject to particular requirements, they differ in construction, type, and operation mode of the sharpener, presence or absence of the unit limiting the pulse duration, etc. In this way, the first picosecond generators with the output voltage in the range 15–50 kV [1, 3, 14, 18, 29] and more powerful devices (e.g., [30–34]) were constructed. The first high-voltage picosecond generators with a chopping gap were developed in the early 1960s [18].

Formation line L_1 is charged by DC or pulsed voltage from source U_0 . After spark gap G_1 is triggered, a nanosecond-front pulse arrives at switch sharpener P_2 and then through transmitting line L_3 it comes to load R_L . The primary nanosecond generator with line L_1 and spark gap G_1 can be replaced by other generators with a nanosecond rise time: a Marks generator, a generator with a semiconductor circuit breaker or magnetic elements, etc. For varying the pulse duration or in the case of unmatched load, one can use chopping gap G_3 . Line L_3 shown in Fig. 5c may be absent; switches S_2 and S_3 are then spatially close [18, 29, 32], which provides a chopping spark gap with ultraviolet illumination.

As was already mentioned, forming and transmitting lines of large diameter cannot be used in the picosecond range because higher wave modes arise that have frequency dispersion and distort the front of the picosecond pulse. Therefore, the experience in constructing the high-voltage nanosecond lines with liquid dielectrics can hardly be realized in most cases. In [9], a coaxial forming line with high-pressure gas insulation was used (see Fig. 6a). A Marks generator charged the line in a short time of 10 ns, which provided the pulse rise time 100 ps and the voltage amplitude up to 400 kV.

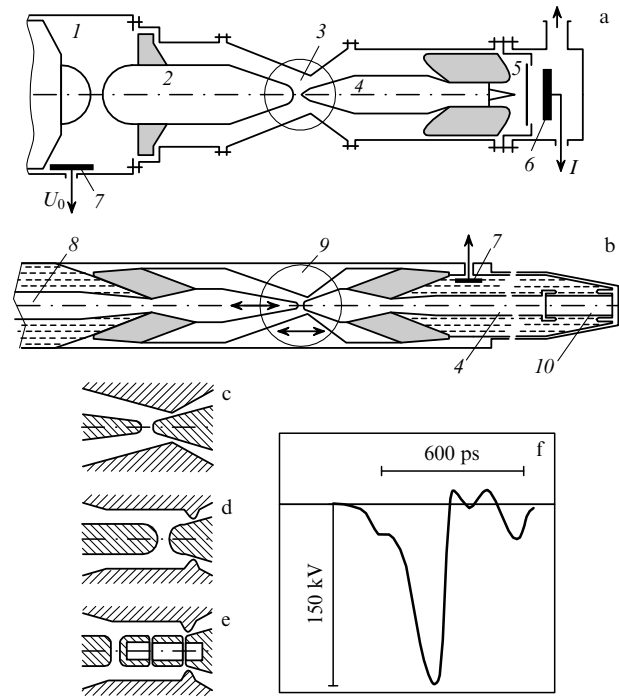


Figure 6. High-voltage picosecond generators with high-pressure nitrogen spark gaps (40–60 bar): (a) generator with a vacuum diode; (b) construction of a shaping slicer with adjustable electrodes; (c–e) various electrode systems of slicer spark gaps; (f) voltage pulse obtained in the slicer with a three-gap sharpening discharge switch; 1 — Marks generator, 2 — formative line, 3 and 9 — sharpening and chopping spark gap units, 4 — transmitting line, 5 — vacuum diode, 6 — beam collector, 7 — capacitive voltage divider, 8 — nanosecond driver output, 10 — resistive load.

A specific feature of the generator shown in Fig. 6a is a common volume for line and spark gaps filled with nitrogen at the pressure 40 atm, which reduces the number of support insulators to a minimum. The pulse duration is shortened by the chopping gap placed near a pulse sharpener. Such a solution allows one to stabilize its operation by the ultraviolet illumination from the sharpener.

The scheme of a pulse generator with an integrated high-pressure gas medium has become central to the development of various compact picosecond systems. With time, the unit combining both the chopping and sharpening gaps has been termed the ‘slicer’. Particular attention was focused on developing systems with adjustable amplitude, duration, and pulse shape that are also capable of operating in a frequency mode (see Fig. 6b). These features of picosecond generators [32, 33] favored their application in studying the formation and dynamics of short electron bunches and generating UHF and super-broadband radio pulses.

For primary impulse nanosecond sources, RADAN-303 generators were used [35]. The gas medium in the slicer was nitrogen at the pressure up to 60 bar. At the energy within the range of 3 J triggered by a spark gap, the rate of nitrogen electric strength recovery provided operation at the repetition frequency up to 25–100 Hz without gap purging. Because the duration of the pulse to be sharpened was 5 ns at the voltage 150–200 kV, the diameter of the slicer’s 50-Ω coaxial line could be minimized to 40 mm, which provided a transmission of a 50-ps pulse front without distortions.

Distortions of the picosecond pulse edge are also reduced if a conventional biconical electrode configuration (see

Fig. 6c) is excluded. Instead, the configuration shown in Fig. 6d) was used with a sufficiently thin disk chopping electrode. In varying gap separations in such schemes, the impedances of nearby sections of the coaxial tract did not change noticeably. In the terminology of wave processes, such a chopping electrode is considered a discrete nonuniformity. The influence of this factor on the pulse front extension was minimized by the numerical simulation performed with code KARAT [36].

The slicer construction was capable of varying gap separations in the course of operation (at the repetition frequency up to 100 Hz) by means of eccentric mechanical actuators. Movement of the grounded chopping electrode was not a problem. A potential sharpening electrode was shifted through a thin insulator placed in the gap separation of the coaxial line filled with gas. At the action time up to 5 ns and the generatrix length 25 mm, the conical insulator withstood a potential up to -400 kV. Gap distances might be adjusted mechanically within an accuracy of $10 \mu\text{m}$, which provides a precise adjustment of the system without dismounting and depressurizing it. The following results were obtained:

- at a constant voltage ramp dU/dt of a picosecond pulse, it is possible to vary the amplitude and duration of the output pulse (the sharpener is fixed and the chopper is adjusted);
- at a constant amplitude, the pulse front duration may be varied (the chopper is fixed and the sharpener is adjusted);
- all three parameters can be varied by adjusting both the chopping and sharpening spark gaps.

The last two items make it possible to vary the shape of the forerunner pulse that arises due to an inter-electrode capacitance of the sharpener. The parameters of the pulse were additionally corrected by varying the number of sharpening gaps (see Fig. 6e), the pressure of nitrogen, and the electrode profiles.

A 160-kV pulse with a half-height duration of 300 ps was obtained in a slicer with a single-gap sharpening spark switch. The pre-breakdown voltage ramp for the sharpening gap was $dU_r/dt = 2 \times 10^{14} \text{ V s}^{-1}$. Because the voltage ramp dU/dt and the gas electrical strength increase in a subsequent spark gap of the slicer, the use of the triple-gap sharpener (see Fig. 6e) allowed obtaining the pulse voltage 150 kV, the pulse half-height duration 150 ps, and the voltage ramp $dU_r/dt = 10^{15} \text{ V s}^{-1}$ (see Fig. 6f). The duration of the pulse tail (50 ps) in this case coincided with the transient character of the recording real-time oscilloscope. The chopping spark gap operated under the ‘traveling wave’ conditions at higher values of dU/dt . Therefore, its gap separation was less than that of the sharpener. In this way, a lower switch inductance was provided and the pulse tail was two or three times shorter than the leading edge, just as it is in the case of the generator shown in Fig. 6a [9]. We note that the trailing edge, in contrast to the leading edge, does not encounter nonuniformities such as a conical or circular chopping electrode.

It was shown that the level of overvoltage across the gap noticeably affects the stability of its switching time. In particular, the switching stability of the chopping gap determines the stability of pulse duration. For example, the oscillograms shown in Fig. 7 were obtained at the output of the slicer by means of a broadband (6 GHz) stroboscopic oscilloscope. This is one of the first employments of stroboscopic technique and proves a sufficient stability of the repetitive signal. If the spread at the instant of chopping gap

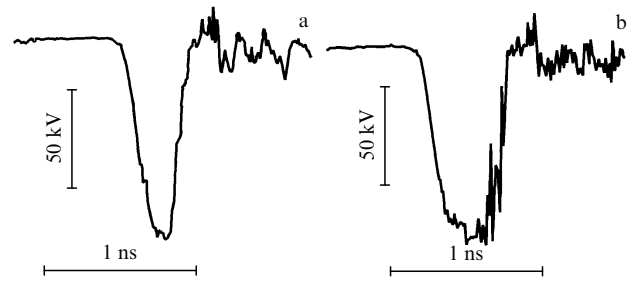


Figure 7. Stroboscopic oscillograms of a slicer pulse obtained at the repetition frequency 100 Hz demonstrate the worse stability of chopping spark gap operation at lower overvoltage across the gap.

switching increased, this was clearly seen as trailing edge jitter on the screen of the stroboscopic oscilloscope (see Fig. 7b), which accumulated 512 trigger events at the repetition frequency 100 Hz.

Data concerning the switching stability dependence on the level of overvoltage allow developing active nano- and picosecond bipolar converters [37–39] with a short forming line and two independent spark gaps (see Fig. 8a). If switches K_1 and K_2 are triggered simultaneously, a symmetric bipolar pulse is formed at the output (see Fig. 8b). The voltage swing across a matched load is then equal to the line charge voltage, which, in equivalent terminology, is twice as great as in the case of the bipolar converter with the parallel shortening line mentioned above (see Fig. 5b).

Study of breakdown mechanisms of untriggered high-pressure spark gaps operating at a high overvoltage made it possible to specify the conditions for obtaining picosecond-accuracy triggering in three-electrode nanosecond high-voltage spark gaps controlled by an electric pulse from an external generator. For example, the 200-kV nitrogen spark gap used in the RADAN-303 nanosecond drivers has a synchronizing accuracy not worse than 300 ps [40], and the energy of the picosecond triggering pulse amounts to 10^{-3} of the switched energy in some cases. It was experimentally shown that a prerequisite to precise switching is the anticipatory breakdown between the gate electrode and the opposite potential electrode induced by the initiating pulse. Deviation at the instant of switching does not exceed the duration of the initiating pulse. It is important that in the precise synchronization mode, the electric field strength at the initiating electrode exceeds 2 MV cm^{-1} . This value is at least three times greater than the breakdown electric field strength in the spontaneous puncture of the gap under the voltage ramp $dU/dt \approx 2 \times 10^{10} \text{ V s}^{-1}$.

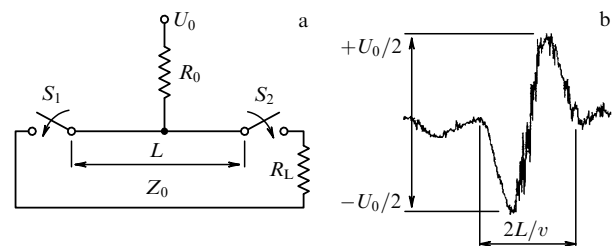


Figure 8. (a) Formation of bipolar pulses in the scheme with two synchronously operating discharge switches. (b) Stroboscopic oscillogram of a bipolar voltage pulse ($U_0 \approx 250 \text{ kV}$) with the duration $2L/v \approx 1 \text{ ns}$ at equal impedances of formative line Z_0 and load R_L .

5. Pulse-periodic picosecond generators

Operation of picosecond generators with spark gaps in a pulse-periodic mode requires that the switches have a short recovery time for electrical strength [41], which is physically determined by the gap deionization time. Plasma deionization occurs faster at the lower energy released in a gas during the discharge. The plasma density is noticeably lower in a volume avalanche discharge than in a discharge with a plasma spark channel. Hence, the regime of volume avalanche discharge provides a shorter deionization time. Anyway, it is reasonable that the cascade preceding a picosecond formation unit would comprise a generator of nanosecond pulses with the shortest possible duration.

Basically, the problem of recovering the electrical strength of the spark gap can be solved by gas circulation, which may totally refresh the working volume in the time lapse between switchings. Unfortunately, at representative gap separations of picosecond switches of the order of 1 mm or less, efficient gas circulation under high pressure is difficult to realize.

As was shown in the previous section, if no precautions are taken, picosecond pulse generators with spark high-pressure nitrogen gaps can operate at the repetition frequency of the order of 100 Hz. This was illustrated in [32, 37–39], where the triggered energy of pulses to be sharpened was not higher than 1–3 J, whereas the power of the formed picosecond pulse was 0.5–1 GW.

At high gas pressure and overvoltage across the gap, the average electric field strength at the cathode of the sharpening spark is always higher than 10^6 V cm⁻¹. Hence, the cathode emits cold emission current from micro-spikes due to an enhanced field, and conditions become suitable for the volume avalanche discharge with multi-electron initiation to arise. The chopping spark gap operates under ultraviolet irradiation from a discharge in the sharpener and the volume discharge in it is also ensured.

A spark gap with an artificially induced volume avalanche switching [42] was a component of one of the first generators of picosecond pulses with a smoothly adjustable amplitude and the repetition frequency up to 10^4 Hz. The switching unit is schematically shown in Fig. 9. The switch was integrated with a storage capacitor. There was an air layer of width 10–30 μm formed by micro spikes on ceramic and cathode plates.

If a pulsed voltage is applied across the electrodes, then a discharge arises at contact points over the ceramic surface. Radiation from the discharge produces cathode electrons,

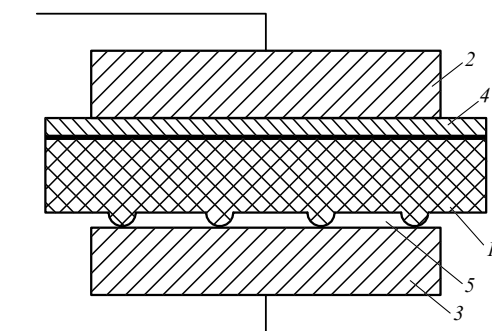


Figure 9. Avalanche gas switch: 1 — pellet from ceramics BaTiO₃, 2 and 3 — metal electrodes, 4 — silver coating, 5 — air gap.

which induce an avalanche discharge in the air gap. Charging voltage pulses with amplitudes up to 2 kV and the front duration 50 ns were preliminarily sharpened by ferrite inductance, which provided a higher voltage ramp in the switch. After the switch is triggered, the current pulse is formed in an output circuit with the half-height duration 0.6 ns. The repetition frequency of the generator was 3×10^4 Hz at the current pulse amplitude 500 A and it was 10^4 Hz at the pulsed current 10^3 A.

The measured deviation of instants at which the current pulse arises on the load was 300 ps and was determined by the instability of the charging source switch. The generator had a power supply that included two thyratrons initiated with a certain relative time shift. It was found that two current pulses could be formed separated by a time lapse up to 1 μs, i.e., corresponding to the equivalent repetition frequency 1 MHz. This generator of picosecond current pulses was used to supply a semiconductor laser diode.

In the kilohertz and higher repetition frequency range, the high-voltage energy storage should be charged to a stabilized voltage with a required periodicity. Hence, the characteristics of the charging unit in many respects determine the performance of the high-power picosecond generator as a whole. If thyratrons and thyristors are used as switches in a primary charging circuit, then the repetition frequency may be 10^4 and higher under the condition that the charging unit is cooled. If a spark gap with high-pressure nitrogen or air is used in the nanosecond stage of energy compression, then an intense gas flow is needed for obtaining the repetition frequency 10^3 Hz, and a controlled start system is required [40, 43–45] for stabilizing the voltage at the level of a few percent.

Stable charging of picosecond capacitive energy storage at repetition frequencies 10^3 Hz and higher can be easily realized if a high-voltage generator (driver) with a completely solid-state switching system is used as a nanosecond charging unit [46]. Several variants of high-power picosecond generators have been made on this basis.

The first variant was a serial two-cascade scheme for forming a picosecond front by the semiconductor diode sharpeners [21, 22] mentioned above. Without gas-discharge switches, such picosecond generators are the most stable among those with the output power 0.5 GW (see Fig. 3b) presently developed.

In the next variant, the duration-adjusted picosecond pulses with the peak power 0.8 GW and repetition frequency up to 3.5 kHz were obtained in a hybrid scheme. A solid-state nanosecond driver of the SM-3NS type [46] with an inductive energy storage and a semiconductor opening switch (SOS) — based current interrupter was combined with a formation unit for picosecond pulses on the basis of a capacitive storage and hydrogen spark gaps at the pressure 100 atm, thus forming a generator. Under the same conditions, hydrogen has a shorter recovery time as compared to other gases. It has, however, a lower electrical strength as compared, for instance, to nitrogen. Hence, the required pressure is 100 atm and more.

The driver provided the output charging pulses with the half-height duration 5 ns at the total amplitude instability less than 1%. The driver pulse charged the formative line of a picosecond converter with the impedance 50 Ω and the capacitance 10 pF. The line was combined with a hydrogen discharge unit. The sharpening and chopping spark gaps could be smoothly adjusted in the course of operation similarly to the slicer considered above [32].

In experiments, the breakdown voltage in the sharpener was adjusted closely to the maximum charging voltage of the formative line (420 kV). Nevertheless, no failures in spark gap triggering were observed. This can be explained by the high stability of the charging pulse and by the fact that in an emergency mode of a statistical breakdown-voltage deviation across the gap, the driver with inductive energy storage automatically raises the voltage to the limiting value determined by the capacitive load. A gap breakdown might occur, albeit with a certain delay, up to a post-triggering in the tail part of the charging curve of the capacitive storage.

At a gas pressure of 100 bar, it is difficult to make a picosecond former with a uniform coaxial tract. Reflections and distortions of amplitude–frequency characteristics are most probable near the chopping electrode and output insulator. To escape considerable nonuniformities near the insulator, the construction was primarily optimized via numeric simulation [36]. Both the numerical model and experiment show that the shortest pulse front of 140–150 ps was obtained without a disk chopping electrode. If it was installed or the chopping gap separation was made smaller, the front of the formed pulse was enlarged to 180–200 ps, and at a short total pulse duration, a certain reduction in the amplitude was observed (see Fig. 10).

In the hybrid picosecond generator described, shape-adjustable pulses were obtained at the 45 Ω output with the amplitude 200 kV, the pulse front shorter than 200 ps, the pulse duration 0.4–1.5 ns, and the repetition frequency up to 3.5 kHz. It was a burst-mode operation with the duration 1–3 s and the interval 3–5 min between packets. The average power in a packet reached 0.7–2.5 kW depending on the pulse duration.

The hybrid scheme was successfully used in creating the most powerful pulse-periodic generator of high-voltage pulses with a picosecond front [48, 49]. A nanosecond driver with a solid-state switching system of the S-5N type was used in this generator [46]. A formative 50 Ω line with the capacitance 70 pF was charged to 900 kV in 40 ns at the average rate $dU/dt \approx 2 \times 10^{13} \text{ V s}^{-1}$. A hydrogen spark gap under the pressure 50 bar without a gas circulation system was used as a switch. The repetition frequency of pulses was 730 Hz. The packet duration was 1 s and the average power over the packet exceeded 25 kW. The pulse formed at the 75 Ω generator output had the duration 7 ns, the amplitude up to –530 kV, and the peak power 3.7 GW. The duration of the pulse front did not exceed 500 ps (see Fig. 11).

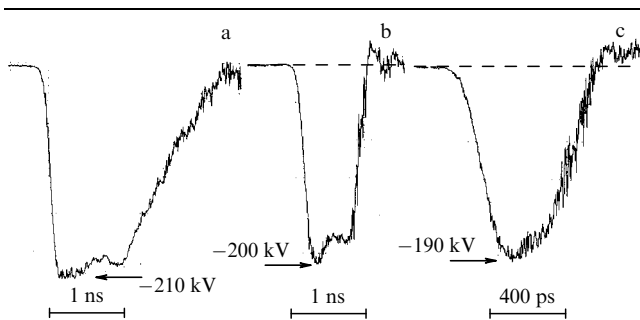


Figure 10. Stroboscopic oscillograms of width-adjusted voltage pulses at the output of a hybrid picosecond generator (45 Ω) [47] with front durations from (a) 150 to (b) 200 ps. The repetition frequency is 1 kHz.

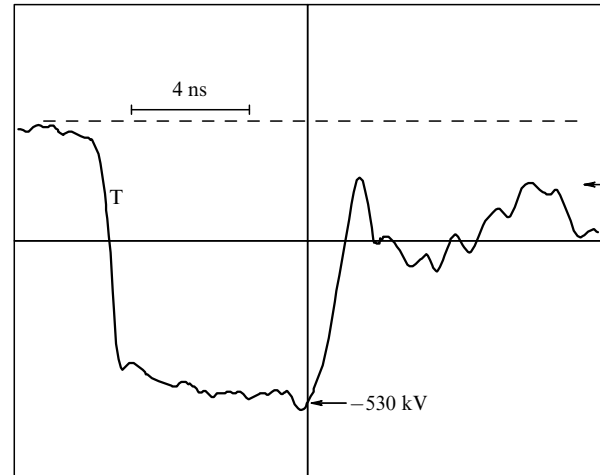


Figure 11. Pulse with the amplitude –530 kV, front duration 500 ps, and half-height duration 7 ns formed by a hybrid high-voltage generator [49] at the repetition frequency 730 Hz.

6. Employment of high-power picosecond pulses

6.1. Picosecond electron diodes

One of the early applications of high-power high-voltage picosecond pulses was the generation of electron bunches in vacuum cold-cathode diodes, which operate on the basis of explosive electron emission [6]. A vacuum diode of the first high-current picosecond electron accelerator is schematically shown in Fig. 6a. A formation technique and the parameters of picosecond accelerating voltage pulses were presented in Section 4. Metal spikes or ends of pipes made from tungsten foil were used as the cathode. An electron bunch with the energy 250–300 keV and the current 2.5 kA at the pulse duration 0.2–0.4 ns was formed in the diode. Later, this method of obtaining picosecond electron bunches was used for electron energies up to 1 MeV [31].

A specificity of vacuum diodes in high-current accelerators operating in the picosecond range is that the capacitance of the anode–cathode system $C_D < t_r/Z$, where Z is the output impedance of the pulse generator. In particular, for $Z = 30 \Omega$, the required capacitance is $C_D < 1 \text{ pF}$ [9]. This condition should be especially taken into account in choosing the cathode construction.

Along with the construction simplicity of a picosecond electron diode, there is one more important feature for forming short bunches, namely, high electron current density. In contrast to nanosecond accelerators, at pulse durations noticeably shorter than 1 ns, one can obtain a diode current higher than 1 kA without plasma overlapping the gap at the anode–cathode separation 0.1–0.2 mm. In this way, high current density can be provided at the anode without special focusing units. For example, with a spike-shaped cathode, an average current density at the anode exceeded 1 MA cm^{-2} at the bunch diameter 0.2–0.3 mm, and in the central part, it exceeded 10 MA cm^{-2} [50]. Correspondingly, a maximum density of bunch power at the anode exceeded $10^{12} \text{ W cm}^{-2}$, which is comparable to the specific parameters mentioned in the Introduction for the most powerful pulsed electron accelerators operating in the range of durations exceeding 10^8 s . At such parameters of the

picosecond electron bunch interacting with the foil anode, the effect of anode material scabbing was found from the side opposite to the direction from which the electrons move. This effect has not been observed before in the range of picosecond pulses.

Another peculiarity of picosecond vacuum electron diodes discovered in the first experiments [9] is the possibility of generating an electron bunch in a low vacuum (of the order 10^{-2} Torr). Moreover, recent experiments show (e.g., [51, 52]) that even at a gas pressure close to atmospheric in diode gaps of a certain configuration, there is no instantaneous overlapping of the gap by a discharge during a picosecond front of high-voltage pulses. In this case, the cold cathode of such a ‘diode-spark’ gap switch may inject a sufficiently intense electron bunch with a current of dozens or hundreds of amperes initiated by explosive electron emission.

Here, seemingly, the regime of continuous electron acceleration (fleeing) [4, 51] is realized, which still requires thorough investigation allowing for new possibilities of modern detecting devices with picosecond resolution. The problem is interesting from the standpoint of obtaining short-duration electron and X-ray pulses in diode gaps at normal gas pressure. It is also interesting to continue studying mechanisms of precise initiation of controlled high-pressure gas spark gaps [40].

In view of short accelerating pulse duration, the problem of generating short-duration high-current electron bunches has an interesting and physically important aspect concerning the explosive cold cathode functioning. It is known [6] that such a cathode can inject nanosecond and longer-duration dense bunches due to the regeneration of elementary centers of explosive electron emission. This is possible if the energy released in Joule heating by the field-emission current and in micro-emitter explosions is sufficient for melting the material in a domain near the cathode and for the next formation of new emitting nonuniformities. They arise because the melted material splashes out under the action of high pressure in the nearby gas–plasma phase.

If the energy release is not sufficient, the ‘buffing’ effect is observed [53], which leads to a smoothing of the micro relief and degradation of the cathode emission properties. It is clear that under the action of picosecond pulses, the ‘buffing’ effect must appear most obviously. If the number of micro-emitters at the cathode is initially limited, then a fall in the emission current may be observed after several switchings. If the cathode surface comprises a great number of ‘potential injectors’, then numerous short-duration ‘buffing’ pulses are needed. In this case, the change in the emission properties is soon manifested in picosecond electron diodes operating at a high repetition frequency.

In [54], properties of an explosive cold pipe graphite cathode were studied. The hybrid picosecond generator [47] mentioned above fed the cathode with packets of pulsed voltage (see Fig. 10a) with the pulse front shorter than 200 ps, the half-height duration 1.5×10^{-9} s, and the repetition frequency varying from 1 to 3.5 kHz. The maximum power of the injected magneto-insulated electron bunch averaged over the packet duration of 1 s exceeded 2.5 kW. The current density averaged over the emission edge of the cathode was 5×10^4 A cm $^{-2}$.

The experiments provided quantitative information on emitter degradation, i.e., on the growth of the emission current delay in an electron bunch versus the charge

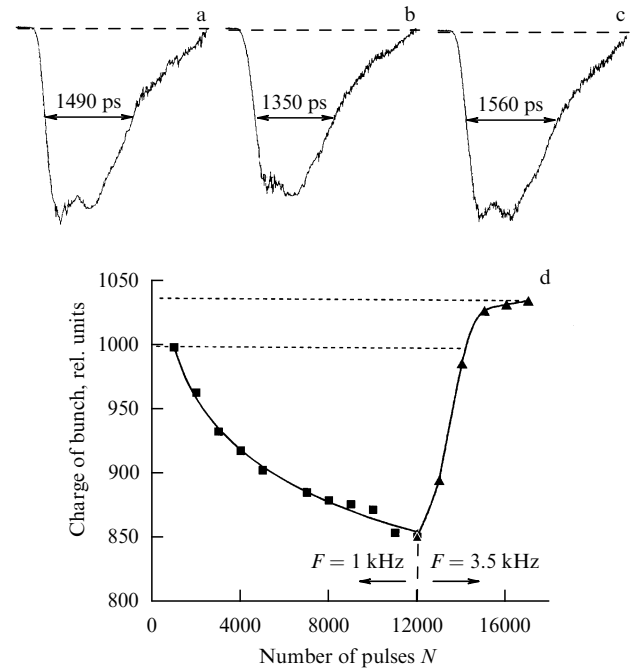


Figure 12. Current pulses of an electron bunch with the amplitude 2 kA: (a) before training, (b) trained by 1.2×10^4 pulses at the repetition frequency $F = 1$ kHz, (c) after additional training by $(1.2-1.7) \times 10^4$ pulses at $F = 3.5$ kHz. (d) Charge variation for the bunch in subsequent training at the repetition frequencies 1 and 3.5 kHz.

transferred. The current in the electron bunch in [54] was detected by a digital stroboscopic oscilloscope with the relative time resolution 10 ps. It was found that the current pulse amplitude duration (see Figs 12a and 12b) and the charge of the emitted beam (see Fig. 12d) steadily fall in the course of cathode training at the pulse repetition frequency 1 kHz and lower.

According to the analytical model developed for the experimental parameters, a single micro-emitter at the cathode edge is completely cooled to the temperature 300 K in a time lapse of the order of one millisecond, which corresponds to the repetition frequency up to 1 kHz. In this case, the micro-geometry of the cathode surface changes (see Figs 13a–13c) in agreement with the ‘buffing’ effect, which results in a greater emission lag time and in a reduction in the charge transferred per pulse.

It turns out that the degradation can be surmounted by increasing the repetition frequency of pulses above a certain critical value (see Figs 12b and 12c). The results of estimations show that the operation at the repetition frequency 3.5 kHz at a sufficient number of pulses per packet yields an increased heating of the cathode material (see Fig. 13d) and, probably, melting. This is possible where the emission in the next pulse arises from a previously heated domain, which, in turn, is facilitated by initiating the Richardson effect.

Accordingly, there are grounds to believe that the ‘buffing’ effect has a certain frequency boundary, i.e., that a regeneration of cathode emission centers while injecting picosecond electron bunches is possible. This result is rather important in practice. Although the regeneration mechanism differs from the nanosecond and longer-duration operation mode, the determining factor, namely, the energy released in the micro-emitter zone, is the same.

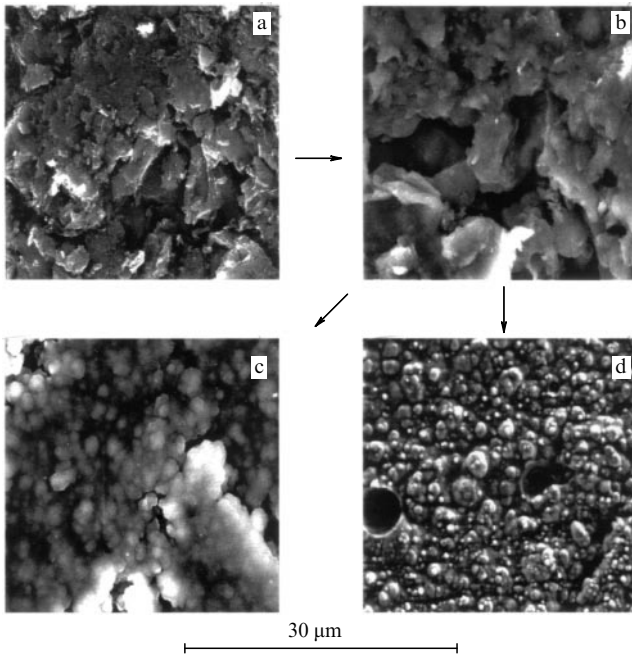


Figure 13. Photograph of an emitting cathode edge: (a) before training, (b) after training by $N = 10^4$ pulses at the repetition frequency $F = 1$ kHz, (c) after additional training by $N = 3 \times 10^4$ pulses at the repetition frequency $F = 1$ kHz, (d) after training by $N = 1.2 \times 10^4$ pulses at $F = 1$ kHz with the next training by $N = (1.2-1.7) \times 10^4$ pulses at $F = 3.5$ kHz.

6.2 Picosecond X-ray sources

Vacuum electron diodes with explosive cold cathodes are widely used for creating high-power sources of picosecond bremsstrahlung pulses with the characteristic quantum energy $10^5 - 10^6$ eV and higher (see [7, 55] and the references therein). Electron bunches with high-power or long-duration current pulses are known to have technical problems concerning overheating of the anode of an X-ray tube usually made from material with a large atomic number (tungsten, tantalum, etc.) and low heat conductivity. In stationary low-current fine-focus tubes, the heat-conduction problem is solved by employing rotating cooled reflecting anodes (see Fig. 14a), whereas a high-power nanosecond-bunch tube requires, instead of a simple shoot-through anode (see Fig. 14b), a reverse reflecting anode (see Fig. 14c), which is used, for example, in well-known nanosecond cold cathode tubes of the IMA series [56] for operating in a pulse-periodic mode. Nevertheless, a system with a reverse anode is also limited by the heat regime and differs in the greater dimensions of the X-ray focus.

Picosecond X-ray sources are mainly useful where high power dose and fine focus are required and the radiation spectrum may be broad. As was mentioned, at a pulse duration of a few hundred picoseconds, a plane-geometry vacuum diode (see Fig. 14b) yields a high current density at the anode, i.e., the diameter of the X-ray focus in such a tube may be 200–300 μm [9] and the energy dissipation in the anode material is not high in this case because of the short pulse duration.

Moreover, the specifics for picosecond range growth of electrical strength of insulators and vacuum gaps mentioned above makes it possible to miniaturize X-ray tubes as well as high-voltage tracts supplying a pulsed voltage. For example, these effects were taken into account in [31] while using

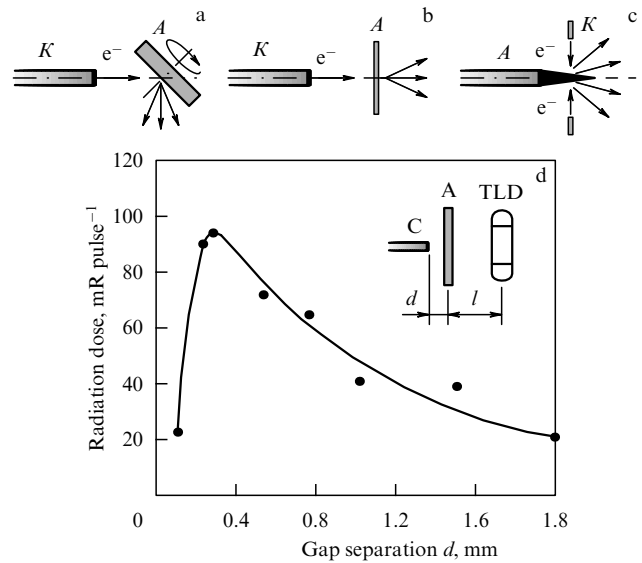


Figure 14. Construction of X-ray tubes: (a) with a massive rotating cooled reflective anode; (b) with a shoot-through thin anode; (c) the reverse tube with a bar reflective anode. (d) Exposition radiation dose of an X-ray tube versus the anode–cathode separation (C—cathode, A— anode, TLD—thermo-luminescence dosimeter, $l = 1$ cm).

commercial nanosecond vacuum diodes IMA2-150D and IMA3-150E for generating electron bunches and X-ray radiation with the amplitude of accelerating picosecond pulses up to -1 MV, whereas at the duration longer than 10^{-8} s, the voltage -200 kV results in the vacuum accelerating gap in such diodes becoming overlapped.

In [9], an original construction of a high-power X-ray source developed on the basis of a high-voltage picosecond generator [30] was suggested and investigated. The main problem was to make the X-ray tube compact. It is seen in Fig. 14e that in a tube connected directly to the generator, the maximum dose per pulse corresponds to the anode–cathode separation $d = 0.2 - 0.5$ mm.

In later experiments, a model of a compact tube was connected to a picosecond generator by segments of the commercial radio-frequency cable with the external conductor diameter down to 7 mm. The cathode geometry was the end of the central conductor of the cable and the anode was made from a tungsten plate. The voltage measured across the tube model and the radiation doses observed at the distance 1 cm from the anode averaged over 50 pulses are presented in the Table. The radiation parameters did not depend on variations in the residual pressure in the tube in the range $10^{-1} - 10^{-3}$ Torr.

It was shown that high-frequency damping in cables of various diameters affects the amplitude attenuation of the picosecond voltage pulse supplying the tube. The insulation electrical strength of the cable with the diameter 4 mm was sufficient for shooting 800–1000 pulses. With the cable diameter enlarged to 7 mm, the accidentproof resource of the feeder at the pulse amplitude 100 kV increased by more than an order of magnitude.

The resource of a picosecond X-ray source can be considerably enhanced if the cable tract is matched with an X-ray tube. No reflected pulses are observed in this case, i.e., the time of high-voltage action on the insulation is reduced and the electron bunch acquires the maximum energy from a

Table. Parameters of picosecond X-ray pulses

Type of cable	Attenuation at the frequency 1 GHz, db m ⁻¹	Length, cm	Voltage across the tube, kV	Dose, m R pulse ⁻¹
RK-75-1, 5-11	1.2	50	45	0.55
RK-50-2-11	0.8	50	56	0.64
RK-754-11	0.4	50	78	5.65
	0.4	80	63	—
RK-75-7-11	0.21	50	124	15.2
	0.21	150	123	—
Without cable	—	—	220	64.2

pulsed generator. Because a vacuum diode has a nonlinear voltage-current characteristic, generally, it cannot be matched with a transmitting line. Nevertheless, such matching can be performed for particular shapes of the voltage pulse. For example, in [57], a method was suggested and the corresponding calculations were performed in the case of a triangular pulse shape at the voltage amplitude 30 kV and the cable impedance 50 Ω. It was shown that the matching is fulfilled for a vacuum diode at the inter-electrode separation 0.11 mm, cathode diameter 0.87 mm, and half-height pulse duration 0.9 ns.

Thus, employing high-voltage picosecond pulses makes it possible to create compact X-ray tubes supplied through segments of a coaxial cable of a relatively small diameter and a length of the order of 1 m. The results presented prove the assumption that such X-ray generators operating at the enhanced frequency of pulses may be used for local surface and intracavitary X-ray therapy.

6.3 Formation of magneto-insulated electron bunches

The experience in the development of picosecond vacuum electron diodes with an explosive cold cathode described above and the created high-voltage pulsed generators made it possible to investigate the formation of magnetized high-current electron bunches with the duration shorter than 1 ns. Such bunches are formed in a coaxial magneto-insulated diode that comprises a paraxial cathode and a female pipe anode. Electrons are emitted from the cathode end and its abutting cylindrical surface, where electric fields are much stronger than in the uniform part of the coaxial line and may reach the value of a few MV cm⁻¹. The anode electrode usually has a contraction with a drift hole. Then an extended drift chamber follows, which, similarly to the cathode, resides in a strong longitudinal magnetic field. Hence, the injected bunch with a prescribed transverse structure can be transported in the drift chamber over distances much longer than the accelerating gap in the diode.

High-current accelerators with moderate-relativistic magnetized bunches of a nanosecond duration were conventionally used for studying the plasma–bunch interaction and generating high-power microwave pulses. It is shown below that picosecond systems of a similar construction have become the most important instruments in a series of new fundamental and applied investigations concerning nonstationary generation modes of super-power microwave pulses. Technically, the creation of picosecond high-current accelerators with magnetized bunches became possible after generators of short-duration accelerating pulses with stable

adjustable parameters had been developed [32] and systems with a repetition frequency of dozens of hertz and higher [47] became available.

We recall that at the cathode voltage -300 kV, the electron relativistic factor is $\gamma = 1.6$ and the velocity of electrons is $0.78c$. Under these conditions, at the pulse duration 300 ps, the spatial length of an ideal bunch is 7 cm. The term ‘ideal’ is used here because the irregular shape of the accelerating pulse and the Coulomb interaction result in an actual pulse shape and duration differing from the envelope curve of the accelerating voltage pulse just at the entrance to the drift chamber. Moreover, the longitudinal structure of the bunch undergoes considerable dynamic variations in the process of transportation. These problems were especially studied in experiments [58], where the installation was based on a nanosecond driver RADAN-303 [35], a picosecond slicer-converter [32], and an accelerating unit that was a coaxial magneto-insulated diode combined with a cylindrical drift chamber (with the diameter 10 mm and length 400 mm), placed in a focusing magnetic field with the intensity 2 T produced by a pulsed solenoid.

The output of the coaxial slicer was matched with a coaxial magneto-insulated diode with the help of a stepwise transmitting line. In this way, the graphite pipe cathode with the diameter 4 mm was supplied by accelerating pulses of up to 250-kV voltage with the duration 300 ps. Slicer tuning provided the possibility to vary, within certain limits, the pulse amplitude, duration, rate of pulse rise, and parameters of the foregoing pulse that arises due to an inter-electrode capacitance in the sharpening gap. When needed, collimators were placed in the anode contraction of the coaxial magneto-insulated diode, which provided a reduction in the electron bunch current from 1 kA to 100 A while not affecting the parameters of the accelerating pulses.

The transverse structure of the picosecond bunch was detected in one pulse by images on a dosimetric film that was placed on a moving collector at various positions inside the drift chamber. The passage of the bunch through a set of films or foils allowed the estimation of the maximum electron energy. A broadband sensor was used for measuring the bunch current [58] with a transient time not worse than 150 ps. The accelerating pulses and sensor signals were recorded by a Tektronix-7250 oscilloscope with the bandwidth 6 GHz and a 10-ps analogue-to-digital converter. The measuring technique and detection methods provided real-time investigations of the dynamics of the electron bunch current pulse. In particular, the time-of-flight analysis of the electron pulse longitudinal velocity was employed.

The important role of the foregoing pulse in the initiation of cathode emission was clarified. Its duration was more critical than the amplitude in general. For example, at a longer time of the foregoing pulse action (see Figs 15a–15c), a greater current and integral charge of the bunch could be obtained even at a shorter duration of the fixed-amplitude accelerating voltage (see Figs 15b–15d).

The longitudinal dynamics of electrons inside a dense bunch prevents the formation of short-duration bunches. In the case of picosecond fronts, fast electrons emitted at a maximum voltage produce a spatial charge. At the input of the drift chamber, this spatial charge additionally accelerates the initially leading low-energy fraction that was injected by the cathode at the accelerating pulse front. In principle, overtaking may occur at this stage. As a consequence, a longitudinal crossover is formed at a distance of 3 cm from the

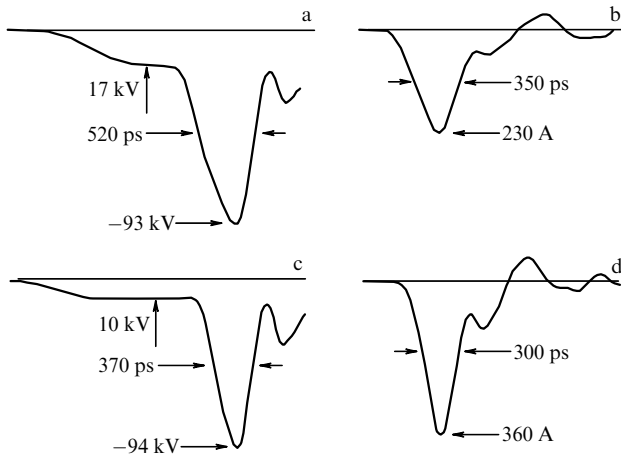


Figure 15. Illustration of the method for initializing a picosecond-range explosive-emission cathode. The shorter-duration accelerating pulse with an extended preliminary pulse (c) provides a higher current and total charge in the picosecond electron bunch (d) as compared to modes (a) and (b), respectively.

cathode (see Fig. 16a), where its structure is most compact. In this case, the amplitude of the current pulse is maximal and its front is sharpened. A longer transportation length results in a fall in the current amplitude, which is accompanied by the corresponding spread of the pulse duration.

In further transporting a pipe-like picosecond bunch with the current amplitude $I \approx 1$ kA and density $j \approx 10^4$ A cm⁻², a considerable additional acceleration of a fraction of the electrons occurred, depending on the drift length. The maximum energy increased by a factor of 1.5 compared to the initial energy of injection to a drift space [58, 59]. These data were obtained by analyzing the depth of shooting dosimetric films and foils with a packet bunch (see Fig. 16b). They qualitatively agree with the velocity of the bunch current front measured by the time-of-flight technique.

The mechanism of additional acceleration might be the auto-acceleration of a fraction of electrons in the field of the spatial charge wave excited in a dense electron bunch. The numerical PIC-simulation [36] yields similar results and shows [59] that the most high-energy fraction of electrons is concentrated at the bunch front. It was also found in experiments and numerical simulation that the increase in electron energy depends on the bunch current at the entry to the drift chamber.

The transverse structure of a short bunch had specific features. Both experiments and a numerical simulation [59] show that the current of a picosecond bunch, strongly reduced by a collimator (by a factor of 5–10), acquired the two-humped shape. The reason was a collimation of electrons emitted from the cylindrical surface of the pipe cathode at the accelerating voltage exceeding a certain value.

Electrons with a small cyclotron orbit radius mainly emitted at the leading and trailing edges of the picosecond accelerating pulse arrived at the drift chamber. A medium ‘high-energy’ portion of the current pulse was most efficiently truncated. In this way, the collimator not only reduced the number of particles with high transverse velocities, but also was a ‘high-energy filter’ capable of qualitatively changing the longitudinal structure of the picosecond electron bunch.

The results concerning injection, formation, and transportation of short high-current electron bunches were used in

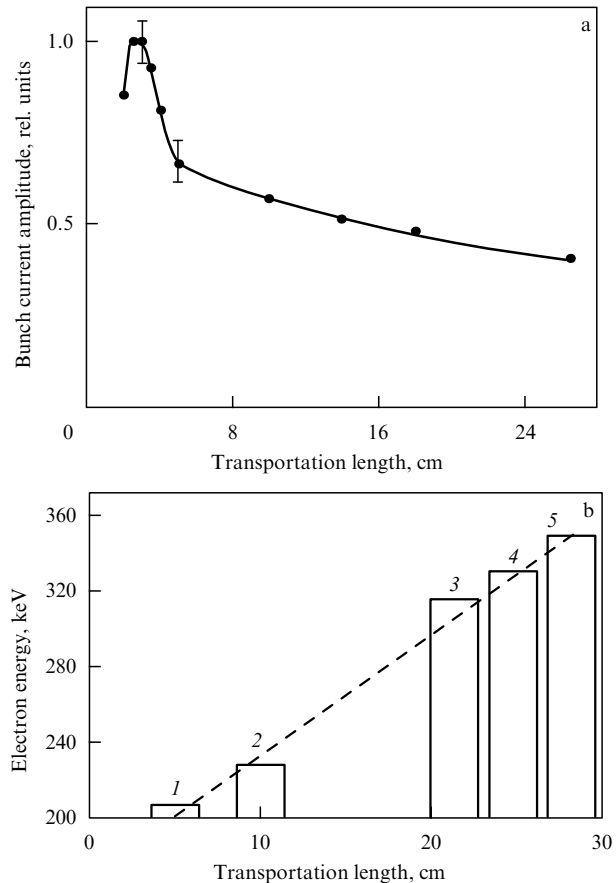


Figure 16. Transformation of the parameters of a tube picosecond electron bunch with the initial energy 200 keV, the current 1 kA, and the duration 300 ps versus the transportation length in the drift chamber of an accelerator with the magnetic field 2 T: (a) the amplitude of the bunch current; (b) the variation of maximum electron energy (1, 4 — experiment; 2, 3, 5 — numerical PIC-simulation).

designing and developing picosecond high-current electron accelerators of the pulse-periodic type. The accelerators based on the nanosecond driver RADAN-303 [60] and a hybrid high-voltage generator [47] had focusing systems in the form of pulsed ($B_z \leq 6.5$ T) or superconducting ($B_z \leq 8$ T) focusing solenoids, in addition to DC solenoids ($B_z \leq 2$ T).

The accelerator with the repetition frequency up to 3.5 kHz [61] injected the electron bunch with the duration 0.4–1.5 ns, the front duration 200 ps, the current greater than 2 kA, the electron energy up to 300 keV, and the power averaged over the packet up to 2.5 kW. Also, a nanosecond installation was created [48] with a picosecond (down to 500 ps) front of the accelerating pulse (see Fig. 11). The electron energy was 600 keV and the bunch current was more than 5 kA. The peak power of the bunch exceeded 3 GW.

6.4 Generation of high-power picosecond microwave pulses

Picosecond high-current accelerators made it possible to study the nonstationary generation of high-power microwave radiation in various UHF devices (see Fig. 17). Mechanisms of induced radiation were considered for short dense fluxes of moderately relativistic electrons in a coherent single-pass mode of amplification of the initial signal that arises at the front of the bunch current pulse. From the practical standpoint, these investigations solve the problems

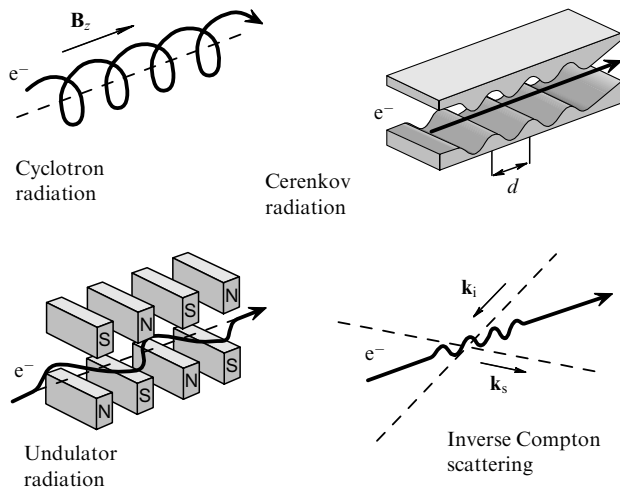


Figure 17. Mechanisms of induced microwave radiation in the high-current moderately relativistic electron bunches studied experimentally by means of high-current picosecond accelerators. For devices based on the effect of electromagnetic radiation scattering, k_i refers to a pumping wave and k_s refers to a scattered wave.

of generating microwave pulses with a duration shorter than 1 ns and of enhancing the level of power conversion of the electron bunch to electromagnetic radiation.

The theory of the cyclotron mechanism for nonstationary generation of picosecond microwave pulses by short electron fluxes [62] was proved experimentally in [63, 64]. Similar operation modes were then studied for devices based on the undulator and Cherenkov microwave radiation [65–67]. By now, the first experimental results have been obtained on realizing the mechanism of backward induced microwave scattering by a picosecond electron bunch. In all these investigations, the high-current picosecond accelerators provided stability and a wide tuning range for the parameters of the electron bunches.

For studying the cyclotron mechanism, a transverse oscillatory velocity was given to electrons of a magnetized bunch with the duration 300 ps at the entrance to a drift chamber by employing the system of short solenoids with opposite coils. The velocity could be adjusted right up to obtaining the pinch factor $g = V_{\perp}/V_z \approx 1$. The possibility of thoroughly measuring the parameters of the electron bunch allowed one to precisely adjust the device.

The UHF radiation was a single pulse obtained under the grazing condition for a dispersion curve. The pulse bifurcates if the dispersion curve is intersected. In this case, the leading-edge frequency exceeded that in the pulse tail (in accordance with the Doppler effect). The radiation power grows exponentially with the interaction length [64]. This is specific to the induced radiation mode. An estimate of the peak radiation power yields 200–400 kW, which corresponds to the bunch energy transformation of 1%.

Picosecond pulses of millimetric waves have also been observed in the case where a short electron bunch passes a drift accelerator chamber in the axial magnetic field combined with the magnetic field of a spiral undulator. A maximum peak radiation power of a few hundred kilowatts was obtained by ‘directly’ switching on the axial magnetic field that reached 1.3 T [65].

UHF pulses with the duration 0.5 ns, the front duration shorter than 200 ps, and the integral (with respect to

frequency) power 1 MW were obtained for a rectilinear bunch (with a current of 100–150 A) interacting with synchronous fields of a dielectric slow-wave system. The transformation efficiency of the bunch energy for such a Cherenkov maser was 3% in the coherent single-pass amplification mode. The device power was doubled if a cascade electro-dynamic slow-wave system was employed, in which an additional section (with the shape of a corrugated waveguide) was installed in front of the dielectric section for modulating the bunch [68].

Most progress in obtaining the high-power picosecond electromagnetic pulses of the millimeter-wavelength range was attained in the experiments with the Cherenkov mechanism of nonstationary UHF generation where a rectilinear high-current bunch passes through a periodic slow-wave structure, provided that electrons were matched to the backward spatial harmonics of the base wave TM_{01} .

It is known that electron UHF devices with such matching (backward-wave tube, BWT) operating with long-duration bunches can yield the sharp initial power overshoot that is a few times greater than the stationary generation level [69]. In minimizing the duration of the electron bunch, i.e., in using picosecond accelerators, this initial stage of the transient process in a relativistic BWT was selected ‘in a pure form’ and thoroughly studied in the frequency ranges of 38 GHz, 70 GHz, and 140 GHz [70].

In experiments [67], a quadratic relation was shown between the radiation pulse peak power and the charge of the electron bunch, which proved the coherent character of radiation from the whole volume of a spatially limited electron flux. If a superconducting magnet was used for focusing the bunch, such a microwave source operated at the repetition frequency 25–100 Hz. In the 8-mm wavelength range, a traditional scheme of a moderately relativistic BWT [71] yields considerably high UHF peak power of the order of 60–150 MW [67, 70], although the power bunch–radiation conversion factor did not exceed 0.3.

In later experiments, modified periodic slow-wave structures of BWTs with an increased transverse dimension were used [72]. In this case, the spatial charge of the bunch does not critically affect the process of electron bunching, the dispersion of a broadband wave packet is lower, and the slow-wave system is a convenient channel for the transportation of electrons. The last factor is of particular importance at a reduced magnitude of the focusing magnetic field. By employing a picosecond accelerator on the basis of the RADAN-303 driver at the induction of the focusing magnetic field 2 T, the UHF pulses were generated with the duration 250 ps and the pulse stuffing frequency 38 MHz. The pulse power was as high as 240–280 MW and the conversion factor was 40–50% [73].

The results obtained gave the possibility to perform the subsequent experiment [61], where the high-current electron accelerator based on a hybrid picosecond voltage pulsed generator [47] was equipped with a cooled DC solenoid ($B_z = 2$ T). Pulses in the 38 GHz range with the peak power up to 300 MW were generated at the repetition frequency 1–3.5 kHz in the packets with the duration 1 s (see Fig. 18a). The radiation power averaged over the packet was as high as 200 W.

The subsequent theoretical study of nonstationary modes of energy exchange in moderately relativistic BWTs, numerical PIC-simulation, and the first experiments with subnanosecond BWTs in the range of 10 GHz at a bunch duration of

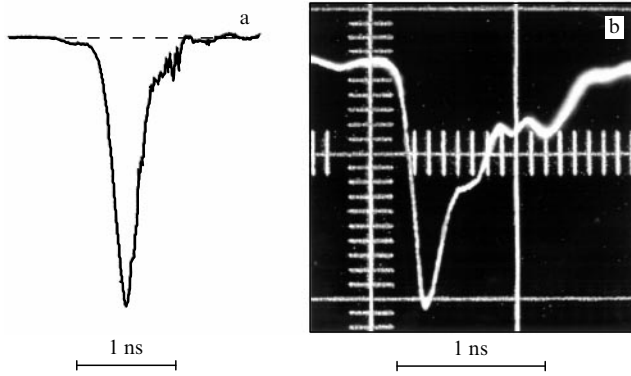


Figure 18. Oscilloscope trace of the envelope of a picosecond pulse of microwave radiation in the range of 38 GHz with the peak power 300 MW detected by an UHF detector and recorded by a stroboscopic oscilloscope at the repetition frequency 1 kHz [61]. (b) Envelope of the pulse from the same range with the peak power 1.2 GW obtained at the bunch power conversion factor 1.5 ± 0.2 [75]. The recording was made by a real-time oscilloscope.

5 ns [74] showed the possibility of generating picosecond microwave pulses with a peak power that would not principally be limited by the power of the electron flux. The basis of this effect is as follows. If a bunch current considerably exceeds the value required for stationary generation, then conditions arise leading to a high increment of the absolute instability of the bunch–wave system. As a result, a short UHF pulse (in the scale of beam extension) is formed that comprises of the order of a dozen or fewer high-frequency oscillations. Moving towards the beam in the slow-wave system, it combines electrons and takes their kinetic energy away in a distributed mode. Such a mode, with a power conversion factor greater than one, gives the opportunity to most efficiently realize potentials of picosecond high-current accelerators.

In experiment [75], the optimized electrodynamic structure BWT in the range of 38 GHz and the pulsed solenoid with the induction 6.5 T provided the conditions under which the power conversion factor for the bunch duration 1 ns was 1.5 ± 0.2 at the output radiation power up to 1.2 GW and the pulse duration 200 ps (see Fig. 18b). The power of the electron beam in this case was 650 MW. The density of radiation power in the electrodynamic structure was 1.5 GW cm^{-2} , which is a record value for an electron UHF device with moderately relativistic high-current bunches. The efficiency of energy conversion in the bunch — electromagnetic wave system was estimated to be of the order of 25% for the microwave source under study.

The experience acquired in employing picosecond accelerators for generating microwave pulses of millimetric waves became an important factor in the investigation and development of similar pulse-periodic sources for the 10 GHz range. In particular, the nanosecond hybrid generator with a picosecond front duration of the voltage pulse [49] mentioned above and the high-current accelerator developed on this basis were used in the experiments on generating radiation in the range of 10 GHz in a packet mode with the duration 1 ns at the repetition frequency up to 730 Hz [48]. The half-height pulse duration did not exceed 800 ps (8 periods of high-frequency oscillations) at the peak power greater than 2 GW. The packet-average radiation power was of the order of 2.5 kW.

It is interesting that the picosecond microwave sources studied in [48, 73–75] were characterized by high electric strength in terms of diffraction systems employed for UHF radiation output to the atmosphere and in a wider aspect. Indeed, the experimental results show that similar devices at a pulse duration of 1 ns are not critically sensitive to a whole class of phenomena (emission processes at the walls in slow-wave systems, secondary emission resonance discharges, etc.), which in high-power nanosecond electronics conventionally limit the duration of generated radiation pulses (see, e.g., [76]).

6.5 Sources of super-broadband radio-frequency radiation

The above examples show that picosecond pulses of UHF gigawatt-power radiation can be generated in electronic devices with relativistic high-current bunches. The pulses of accelerating voltage are then transferred from a high-voltage generator to a vacuum accelerating diode through a coaxial line as a TEM-wave, and only after the bunch injection is their energy converted to the energy of electromagnetic radiation. The total efficiency of such sequential energy conversion is not high; it depends on the radiation wavelength and varies from unity to two–three dozen percent.

The energy of a TEM-wave of a high-voltage picosecond generator can also be converted to electromagnetic radiation without employing the electron bunch as an intermediate agent, namely, by the direct emission of an electromagnetic pulse through a super-broadband TEM-antenna (see, e.g., [11, 77]). As far as the range of durations of pulses exciting the antenna is concerned, it is obvious from general reasoning that the pulsed power of such an emitter increases at a shorter duration of current drops in the antenna. Thus, the use of picosecond pulses seems promising.

The properties of sources with a pulsed excitation of the antenna considerably differ from the corresponding characteristics of similar-duration pulses with UHF stuffing and substantially depend on the pulse duration. The frequency spectrum width Δf defined as $\Delta f = f_{\max} - f_{\min}$ can be sufficiently large in this case and comparable with the mean frequency $f_0 = (f_{\max} + f_{\min})/2$, where f_{\max} and f_{\min} are the high and low frequency boundaries of the pulse spectrum. According to the classification given in [11], the radiation generated by an antenna excited by short-duration pulses without HF stuffing is super-broadband (SBB) if $\Delta f/f_0 \geq 1$ holds.

The frequency spectrum width Δf is determined by the pulse duration t_p , the pulse rise time t_r , and, in the wide sense, by the pulse shape. According to [78], the frequency $f_{\max} \approx 0.4/t_r$. At the pulse duration $10^{-9} - 10^{-10}$ s, the value of Δf is within the gigahertz frequency range. High-power SBB generators with such radiation characteristics are interesting for performing reliability tests of electronic devices and for pulsed radar systems.

SBB generators have certain specific features. The main one is that the shape of the emitted SBB pulses differ from those of the voltage pulse passed to the antenna input. One more factor that distorts the emitted pulse is the finite frequency bandwidth of the TEM-antenna that can be presented as a band-pass filter. Hence, for reducing shape distortions in the emitted pulse and enhancing the energy efficiency of the radiator, it is necessary to employ the exciting pulses with the spectrum whose energy is mainly concentrated in the frequency band corresponding to the antenna transmission band. In this respect, the shape of the pulse exciting the

antenna is important. For example, a unipolar pulse has a spectrum with the maximum in low frequencies, which the antenna cannot radiate and which are reflected from the antenna–feeder junction. Bipolar pulses, whose spectral function tends to zero in the low-frequency limit, are more efficiently emitted. Formative methods for high-power picosecond bipolar pulses were discussed earlier.

Presently, high-power picosecond SBB pulses are emitted mainly by three types of antennas: a horn TEM-antenna [79, 80], antennas with a parabolic reflector, termed IRA (Impulse Radiating Antenna) [81, 82], and combined antennas [83]. Sources of SBB pulse radiation can be conventionally separated into systems with a single antenna and pulse array antennas. The latter type is interesting for radar applications.

Horn TEM-antenna sources of high-power radiation [33, 80, 84] were excited by unipolar and bipolar picosecond pulses. In using longer-duration pulses (more than 1 ns), the power at the input of such an antenna may be as high as 10 GW. An image of a single horn TEM-antenna is shown in Fig. 19a. The exciting pulse for the antenna passes through a feeder. If the feeder is coaxial, then the antenna is matched by a coaxial–strip junction.

In the case of a high-power exciting pulse, the antenna–feeder junction may be filled by a dielectric [84]. We note that in the case of picosecond pulses, additional insulation may be unnecessary. For example, it was shown in [33] that at the pulse duration reduced to 200 ps, the electrical strength of air rises to 150 kV cm^{-1} (see Fig. 20), which relates to the growth of the insulation strength in the picosecond range mentioned above.

The voltage amplitude at the input of a TEM-antenna with air insulation could be increased up to 100 kV at the repetition frequency up to 100 Hz [80]. Thus, a compact picosecond generator comprising an air feeder of diameter 36 mm and a horn TEM-antenna were created. They provided the electric field strength 140 V cm^{-1} at the distance of 25 m along the principal direction of radiation. Investigations performed now reveal some drawbacks to horn TEM-antennas. These are a large length compared to the spatial

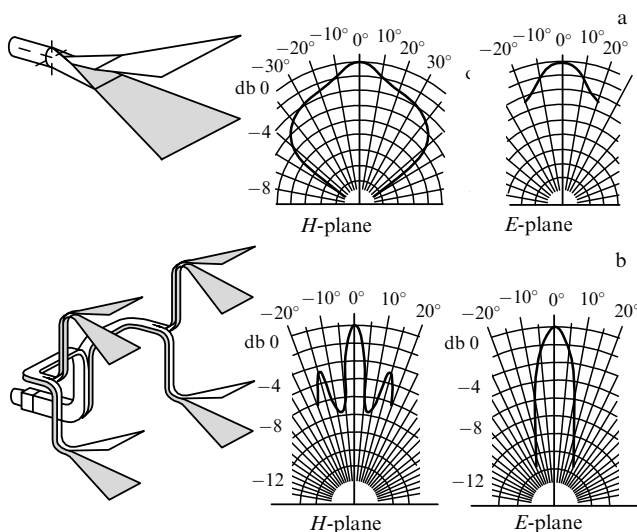


Figure 19. Single TEM-horn with the aperture $30 \times 40 \text{ cm}$ and its directional diagram in the H - and E -planes. (b) Four-antenna radiating system combined from in-phase TEM-horns with the base $135 \times 50 \text{ cm}$ and its directional diagram in the H - and E -planes.

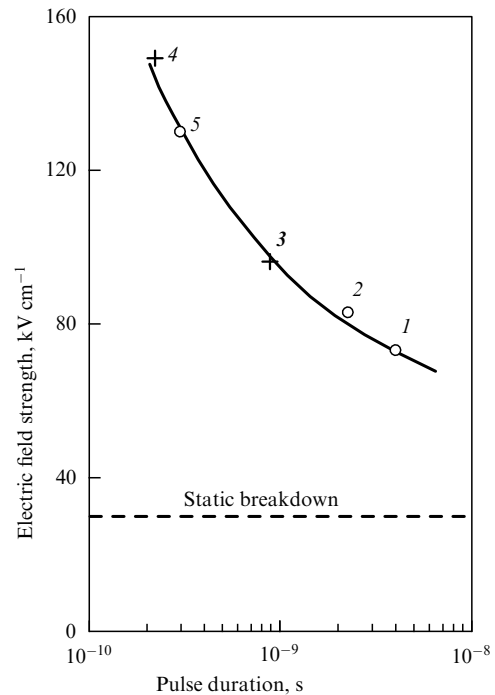


Figure 20. The electrical strength of air versus the duration of the affecting high potential: 1, 2, 5 — UHF pulses in the 38-GHz range; 3, 4 — unipolar voltage pulses without UHF filling.

extension of the exciting pulse, a dependence of the antenna phase center position on frequency, and a wide directional diagram (see Fig. 19a).

High directivity of radiation is specific for picosecond SBB generators based on IRAs with a parabolic reflector. For example, the width of the radiation directional diagram for an IRA with the diameter 4 m [82] is better than 2° . A miniature sharpening hydrogen spark gap at the pressure 100 atm placed in the reflector focus inside a dielectric lens was used in such an SBB source of radiation. Its characteristic time is 130 ps, and the spherical TEM-wave directed to the reflector by two V-type strip-line feeder antennas is formed at the inter-electrode potential 120 kV. Similarly to other SBB antenna types, its radiation spectrum in the principal direction and, consequently, the pulse duration depend on the distance from the radiating aperture due to the dependence of the angular divergence θ on the wavelength λ as $\theta \propto \lambda/D$ (where D is the diameter of the radiating aperture).

We note that the scheme employed in [82] for exciting IRAs by a picosecond front of a pulse current at a long total pulse duration introduces problems of electrical strength and deteriorates the total energy efficiency. Nevertheless, at the distance $L = 305 \text{ m}$ along the principal direction of the SBB radiator, the measured electric field strength was $E = 42 \text{ V cm}^{-1}$. The corresponding characteristic parameter $L \times E$ in this case was 1280 kV.

The technique of forming narrow directional diagrams for monochromatic radio-frequency sources employs the well-known active phased arrays widely used in radar stations [85]. Concerning sources of SBB pulses with several passive radiating pulsed-excited antennas, the term ‘phasing’ can be associated with ‘synchronizing’. A higher directivity and power of a pulsed array is provided by the synchronous summation of fields from separate sources at the observation point. Ideally, the field superposition determines a quadratic

increase in power density with the number of radiators. An obvious requirement for pulsed array operation is the possibility of synchronizing similar exciting pulses to an accuracy comparable to or exceeding the pulse front duration.

Sharpening the radiation directional diagram by means of a phased array (with the linear aperture $D_{\Sigma} = nd_i$, where d_i is the dimension of the unit antenna) is, to a certain extent, equivalent to the growth of the unit radiator directivity by enlarging its aperture to the value $D_1 = D_{\Sigma}$. This can be seen, for example, by comparing the parameters of an SSB generator with the reflecting antenna IRA-4 mentioned above and those of other devices of the same laboratory (GEM-II [84]), which is the two-dimensional (2×2 m) system comprising 144 TEM-horn-antennas fed by stepwise pulses with a 17-kV voltage drop and a duration of approximately 100 ps.

Synchronous switching of capacitive energy storage with an accuracy of 10 ps was provided by optically controlled gallium arsenide BASS's (Balky Avalanched Semiconductor Switches). The system was synchronized by a split laser pulse. Such an array provided the electric field strength $E = 220 \text{ V cm}^{-1}$ at the distance $L = 75 \text{ m}$ with short-term switching at the repetition frequency up to 3 kHz. The characteristic parameter in this case was $L \times E = 1650 \text{ kV}$. One can see that a considerable increase in the total aperture of pulsed arrays compared to the characteristic radiation wavelength results in a high field strength even at a moderate-voltage picosecond pulse supplying a separate TEM-antenna.

The possibility was mentioned [40] to synchronize drivers of the RADAN type within an accuracy of 300 ps. Such switching accuracy makes it possible to create pulsed SBB radiator-arrays with parallel unit elements fed by independent high-voltage generators. The power supplied to the TEM-antenna in each channel may be a few hundred megawatts. Interesting possibilities are connected with the development of the multichannel picosecond sources of similar power on the basis of semiconductor switch-peakers that operate on the principle of forming a tunneling-assisted impact ionization front [22–24].

It was shown in [37–39, 86] that the directivity of SBB radiation can be enhanced in systems of the pulsed array type in which the feed from a single high-power picosecond generator is split and the pulses pass to individual antennas. In this case, a precise synchronization between numerous channels is not necessary, and the requirements imposed on the feeder electrical strength are lower. At a picosecond pulse duration, it is easier to fulfill the condition of isochronal operation for local radiating centers in the antenna system. For splitting the pulse, strip-line [37, 86] or coaxial [38, 39] power dividers are required.

Strip tracts were employed in demonstration experiments, where a picosecond pulse was routed to two [37] or four [86] antennas (see Fig. 19b). Antennas could be connected in antiphase, which provided the formation of a bidirectional radiation diagram. In this case, the signal polarity in the directional lobes is different, which makes it possible to select the signals reflected from objects in both directions. The angular range of the directional diagram of a double in-phase antenna by an amplitude drop of -6 dB was constricted a few times, i.e., to $\pm 5-6^\circ$ compared to a single radiator (see Fig. 19a).

In experiments [39], an SBB source with an enhanced radiation directivity included a bipolar generator of pulses with the voltage drop duration 0.7 ns. The device based on a

nanosecond driver of the type described in [45] was capable of long-term operation at the repetition frequency 100 Hz. The total amplitude excursion of the bipolar pulse on a 50Ω coaxial output was 460 kV. After passing the matching exponential line with the impedance drop from 50 to 3.125Ω , this pulse split into 16 channels and fed individual combined antennas [83] through 50Ω cable tracts of equal length. The combined antennas formed a pulsed array from 16 elements $1.2 \times 1.2 \text{ m}$ in size. The parameters of bipolar pulses with a total amplitude excursion of 110 kV were the same at all inputs of the antennas.

Measurements of fields of radiated TEM-waves show that even if the duration of a bipolar pulse swing is close to 1 ns, the characterizing parameter $L \times E = 1680 \text{ kV}$ for this compact SBB radiator [39] is not smaller than for much more complicated systems [82, 84] excited by pulses with a front duration shorter than 150 ps.

7. Conclusion

The extensive variety of existing and perspective applications of picosecond generators of pulsed voltage, electron bunches, and electromagnetic radiation could not be the subject of consideration in this review for good reason. We have restricted ourselves mainly to the problems of creating high-power picosecond systems as such. Nevertheless, the modern state of investigations and the completeness of presented developments allow qualifying picosecond high-power electronics as an established field of technical physics.

The most substantial 'base' result of the last decade may be the improvement of formation methods for high-voltage picosecond voltage pulses with adjusted parameters such as the amplitude, duration, pulse front, and shape. This resulted from the study of conditions for fast and stable switching in high-pressure gas spark gaps and high-current semiconductor diode structures. Their individual and cooperative employment resulted in the creation of voltage generators with a total pulse duration of a hundred picoseconds and a front duration shorter than 1 ns that provide a peak power of a few hundred megawatts to a few gigawatts on a load at the average power of the kilowatt level in high-repetition-frequency mode.

Among the created picosecond systems, there is a sufficiently large number of compact, essentially desk laboratory devices operating at repetition frequencies of several to dozens of hertz. It was these devices that determined fast and efficient investigations on forming short-duration electron bunches with high current density, generating short-duration X-ray, microwave, and super-broadband radio-frequency radiation. They were used in real-time mode for studying the dynamics of emission processes in cold cathodes and features of the transportation of dense magneto-insulated bunches in the drift channels of high-current accelerators.

Usually, all such results were quickly scaled to more powerful systems. This has been a contributing factor toward further progress in generating super-broadband picosecond radio pulses and creating corresponding radiators with higher directivity. Sources of short-duration microwave pulses of millimetric and centimetric waves with the peak power exceeding one gigawatt arose. At high repetition frequencies, the corresponding average radiation power reaches a few kilowatts.

These parameters are unique if we recall that the pulse envelope at the half-height level comprises no more than ten

high-frequency periods. Such microwave sources in their class are specific to the sufficiently high energy conversion efficiency of the bunches. Moreover, the history of their investigations has stimulated a theoretical substantiation and experimental detection of rather interesting modes of the nonstationary generation of picosecond UHF pulses with the power conversion coefficient greater than unity in the bunch — electromagnetic wave system.

It is not only the relatively low pulse energy that determines the compactness that is specific to high-power picosecond devices. A multiple rise in the electrical strength of high-potential elements in transition to the range of durations shorter than 1 ns plays a considerable or even the determining role. By ‘elements’, we imply a wide class of insulating materials as well as devices. Typical examples are vacuum electrodynamic slow-wave systems of microwave sources mentioned above with a record density of radiation power, thin feeders of high-voltage X-ray sources, super-broadband antenna systems, etc.

Prospects for further investigation and developments in the field of high-power picosecond electronics is still related to the improvement of methods for electrical energy compression. The effective power can be increased by the synchronous summation of pulses from several sources on a load. Such multichannel generators are of particular practical interest. However, many problems are still unsolved. It is worth noting a peculiarity of employing picosecond pulses that consists in a nonthermal character of high-power electromagnetic pulse interaction with the object under study. In this sense, picosecond electronics is contributing to interdisciplinary fields: medicine, biology, chemical kinetics, radio engineering applications, etc.

We are grateful to our colleagues/coauthors for long-term fruitful cooperation. Especially important are works since the early 1990s, which, despite the known difficulties, have been carried out due to support in the framework of the task program of the Presidium of the RAS and RFBR grants (95-02-04791-a; 98-02-17308-a; 99-02-16462-a; 01-02-17029-a; 04-02-16576-a). The interest shown in this study by the international scientific community is one more important factor.

References

- Mesyats G A *Generirovanie Moshchnykh Nanosekundnykh Impul'sov* (Generation of High-Power Nanosecond Pulses) (Moscow: Sov. Radio, 1974)
- Mesyats G A *Impul'snaya Energetika i Elektronika* (Pulsed Power Engineering and Electronics) (Moscow: Nauka, 2004)
- Fletcher R C *Rev. Sci. Instrum.* **20** 861 (1949)
- Korolev Yu D, Mesyats G A *Fizika Impul'snogo Proboya Gazov* (Physics of Pulsed Gas Breakdown) (Moscow: Nauka, 1991)
- Mesyats G A, Proskurovskii D I *Impul'snyĭ Elektricheskiĭ Rasryad v Vakuume* (Pulsed Electrical Discharge in Vacuum) (Novosibirsk: Nauka, 1984) [Translated into English (Berlin: Springer-Verlag, 1989)]
- Mesyats G A *Explosive Electron Emission* (Ekaterinburg: URO-Press, 1998)
- Tsukerman V A, Tarasova L V, Lobov S I *Usp. Fiz. Nauk* **103** 319 (1971) [*Sov. Phys. Usp.* **14** 61 (1971)]
- Mesyats G A, in *Relyativistskaya Vysokochastotnaya Elektronika* (Vyp. 4, Ed. A V Gaponov-Grekhov) (Gor'kiĭ: IPF AN SSSR, 1984) p. 193
- Koval'chuk B M, Mesyats G A, Shpak V G *Prib. Tekh. Eksp.* (6) 73 (1976)
- Glebovich G V (Ed.) *Issledovanie Ob'ektov s Pomoshch'yu Pikosekundnykh Impul'sov* (Moscow: Radio i Svyaz', 1984)
- Astanin L Yu, Kostylev A A *Osnovy Sverkhshirokopolosnykh Radiolokatsionnykh Izmerenĭ* (Fundamental Super-Broadband Radar Measurements) (Moscow: Radio i Svyaz', 1989)
- Mesyats G A, Bychkov Yu I, Kremnev V V *Usp. Fiz. Nauk* **107** (2) 201 (1972) [*Sov. Phys. Usp.* **15** 282 (1972)]
- Grekhov I V, in *Fizika i Tekhnika Moshchnykh Impul'snykh Sistem* (Ed. E P Velikhov) (Moscow: Energoatomizdat, 1987) p. 237
- Fletcher R C *Phys. Rev.* **76** 1501 (1949)
- Felsenthal P, Proud J M *Phys. Rev.* **139** A1796 (1965)
- McDonald D F, Benning C J, Brient S J *Rev. Sci. Instrum.* **36** 504 (1965)
- Morugin L A, Glebovich G V *Nanosekundnaya Impul'snaya Tekhnika* (Nanosecond Pulsed Technique) (Moscow: Sov. Radio, 1964)
- Vorob'ev G A, Mesyats G A *Tekhnika Formirovaniya Vysokovol'tnykh Nanosekundnykh Impul'sov* (Formation of High-Voltage Nanosecond Pulses) (Moscow: Gosatomizdat, 1963)
- Balabin A I et al. *Zh. Tekh. Fiz.* **41** 1675 (1971)
- Schelev M Ya, Richardson M C, Alcock A J *Rev. Sci. Instrum.* **43** 1819 (1972)
- Alichkin E A et al. *Prib. Tekh. Eksp.* (4) 106 (2002) [*Instrum. Exp. Tech.* **45** 535 (2002)]
- Rukin S N et al., in *IEE Materials of Pulsed Power Seminar* (Leicestershire, UK: Loughborough Univ., 2003) p. 3/1
- Rodin P et al. *J. Appl. Phys.* **92** 958 (2002)
- Rodin P et al. *J. Appl. Phys.* **92** 1971 (2002)
- Mesyats G A *Vestn. Akad. Nauk SSSR* (2) 37 (1979)
- Glebovich G V, Kovalev I P *Shirokopolosnye Linii Peredachi Impul'snykh Signalov* (Broadband Transmission Lines for Pulsed Signals) (Moscow: Sov. Radio, 1973)
- Movshevich B Z, Smorgonskiĭ A V *Radiotekh. Elektron.* **29** 1696 (1984)
- Koval'chuk B M, Kremnev V V, Mesyats G A *Dokl. Akad. Nauk SSSR* **191** 76 (1970)
- Heard H G *Rev. Sci. Instrum.* **25** 454 (1954)
- Mesyats G A, Shpak V G *Prib. Tekh. Eksp.* (6) 518 (1978)
- Zhel'tov K A *Pikosekundnye Sil'notochnye Elektronnyye Uskoriteli* (Picosecond High-Current Electron Accelerators) (Moscow: Energoatomizdat, 1991)
- Mesyats G A et al. *Proc. SPIE* **2154** 286 (1994)
- Mesyats G A et al., in *Ultra-Wideband, Short-Pulse Electromagnetics 4* (Eds E Heyman, B Mandelbaum, J Shiloh) (New York: Kluwer Acad./Plenum Publ., 1999) p. 1
- Prather W D et al., in *Digest of Technical Papers: 12th IEEE Intern. Pulsed Power Conf., Monterey, Calif., USA, June 27–30, 1999* (Eds C Stallings, H Kirbie) (New York: IEEE, 1999) p. 185
- Shpak V G et al. *Prib. Tekh. Eksp.* (1) 149 (1993) [*Instrum. Exp. Tech.* **36** 106 (1993)]
- Tarakanov V P *User's Manual for Code KARAT* (Springfield, VA: Berkeley Research Associates, Inc., 1992)
- Shpak V G et al., in *Digest of Technical Papers: 10th IEEE Intern. Pulsed Power Conf., Albuquerque, New Mexico, USA, July 3–6, 1995* (Eds W L Baker, G Cooperstein) (New York: IEEE, 1995) p. 539
- Andreev Yu A et al. *Prib. Tekh. Eksp.* (5) 72 (1997) [*Instrum. Exp. Tech.* **40** 651 (1997)]
- Koshelev V I et al., in *Proc. of the 13th Intern. Symp. on High Current Electronics, Tomsk, Russia, 23–30 July 2004* (Tomsk, 2004) p. 258
- Shpak V G, Shunailov S A, Yalandin M I, in *Digest of Technical Papers: 10th IEEE Intern. Pulsed Power Conf., Albuquerque, New Mexico, USA, July 3–6, 1995* (Eds W L Baker, G Cooperstein) (New York: IEEE, 1995) p. 666
- Meek J M, Craggs J D *Electrical Breakdown of Gases* (Oxford: Clarendon Press, 1953) [Translated into Russian (Moscow: IL, 1960)]
- Koval'chuk B M, Mesyats G A *Prib. Tekh. Eksp.* (5) 102 (1970)
- El'chaninov A S et al. *Prib. Tekh. Eksp.* (4) 162 (1979)
- Bykov N M et al. *Prib. Tekh. Eksp.* (6) 96 (1988)
- Gubanov V P, Korovin S D, Stepchenko A S *Prib. Tekh. Eksp.* (1) 95 (1997) [*Instrum. Exp. Tech.* **40** 85 (1997)]
- Rukin S N *Prib. Tekh. Eksp.* (4) 5 (1999) [*Instrum. Exp. Tech.* **42** 439 (1999)]

47. Lyubutin S K et al. *Prib. Tekh. Eksp.* (5) 80 (2001) [*Instrum. Exp. Tech.* **44** 644 (2001)]
48. Korovin S D et al. *Pis'ma Zh. Tekh. Fiz.* **30** (17) 23 (2004) [*Tech. Phys. Lett.* **30** 719 (2004)]
49. Yalandin M I et al., in *Proc. of the 13th Intern. Symp. on High Current Electronics, Tomsk, Russia, 23–30 July 2004* (Tomsk, 2004) p. 153
50. Mesyats G A, Shpak V G *Pis'ma Zh. Tekh. Fiz.* **3** 708 (1977)
51. Tarasenko V F, Yakovlenko S I V *Usp. Fiz. Nauk* **174** 953 (2004) [*Phys. Usp.* **47** 887 (2004)]
52. Tarasenko V F et al. *Pis'ma Zh. Tekh. Fiz.* **29** (21) 1 (2003) [*Tech. Phys. Lett.* **29** 879 (2003)]
53. Juttner B, Putschkarjov V F, Rohrbech W, in *Proc. of the 7th Intern. Symp. on Discharges and Electrical Insulation in Vacuum, Novosibirsk* (Novosibirsk, 1976) p. 189
54. Korovin S D et al. *Pis'ma Zh. Tekh. Fiz.* **30** (19) 30 (2004) [*Tech. Phys. Lett.* **30** 813 (2004)]
55. Mesyats G A et al. *Moshchnye Nanosekundnye Impul'sy Rentgenovskogo Izlucheniya* (High-Power Nanosecond X-Ray Pulses) (Moscow: Energoatomizdat, 1983)
56. Dron' N A, in *Sil'notochnye Impul'snye Elektronnye Puchki v Tekhnologii* (Ed. G A Mesyats) (Novosibirsk: Nauka, 1983) p. 129
57. Mesyats G A *Pis'ma Zh. Tekh. Fiz.* **28** (13) 36 (2002) [*Tech. Phys. Lett.* **28** 550 (2002)]
58. Shpak V G et al. *Pis'ma Zh. Tekh. Fiz.* **22** (7) 65 (1996) [*Tech. Phys. Lett.* **22** 297 (1996)]
59. Yalandin M I et al., in *Proc. of the 17th Intern. Symp. on Discharges and Electrical Insulation in Vacuum, Berkeley, CA, USA, July 21–26, 1996* Vol. 2 (Piscataway, NJ: IEEE, 1996) p. 635
60. Shpak V G et al., in *BEAMS'96: Proc. of the 11th Intern. Conf. on High Power Particle Beams, Prague, Czech Republic, June 10–14, 1996* Vol. 2 (Eds K Jungwirth, J Ullschmied) (Prague: Inst. of Plasma Phys. Acad of Sci. of the Czech Republic, 1996) p. 913
61. Grishin D M et al. *Pis'ma Zh. Tekh. Fiz.* **28** (19) 24 (2002) [*Tech. Phys. Lett.* **28** 806 (2002)]
62. Ginzburg N S, Zotova I V, Sergeev A S *Pis'ma Zh. Tekh. Fiz.* **60** 501 (1994) [*Tech. Phys. Lett.* **60** 513 (1994)]
63. Ginzburg N S et al. *Pis'ma Zh. Eksp. Teor. Fiz.* **63** 322 (1996) [*JETP Lett.* **63** 331 (1996)]
64. Ginzburg N S et al. *Phys. Rev. Lett.* **78** 2365 (1997)
65. Ginzburg N S et al. *Izv. Vyssh. Uchebn. Zaved., Prikl. Nelin. Din.* **6** (1) 38 (1998)
66. Ginzburg N S et al. *Zh. Tekh. Fiz.* **72** (3) 53 (2002) [*Tech. Phys. Lett.* **47** 335 (2002)]
67. Ginzburg N S et al. *Phys. Rev. E* **60** 3297 (1999)
68. Yalandin M I et al. *Pis'ma Zh. Tekh. Fiz.* **23** (24) 14 (1997) [*Tech. Phys. Lett.* **23** 948 (1997)]
69. Ginzburg N S, Kuznetsov S P, Fedoseeva T N *Izv. Vyssh. Uchebn. Zaved., Radiofiz.* **21** 1037 (1978) [*Radiophys. Quantum Electron.* **21** 728 (1978)]
70. Yalandin M I et al. *IEEE Trans. Plasma Sci.* **PS-28** 1615 (2000)
71. Kovalev N F et al. *Pis'ma Zh. Eksp. Teor. Fiz.* **18** 232 (1973) [*JETP Lett.* **18** 138 (1973)]
72. Korovin S D et al. *Izv. Vyssh. Uchebn. Zaved., Radiofiz.* **42** 1189 (1999) [*Radiophys. Quantum Electron.* **42** 1047 (1999)]
73. Klimov A I et al. *IEEE Trans. Plasma Sci.* **PS-30** 1120 (2002)
74. Eltchaninov A A et al. *Laser Part. Beams* **21** 187 (2003)
75. Korovin S D et al. *Pis'ma Zh. Tekh. Fiz.* **30** (3) 68 (2004) [*Tech. Phys. Lett.* **30** 117 (2004)]
76. El'chaninov A S et al. *Pis'ma Zh. Tekh. Fiz.* **7** 1168 (1981) [*Tech. Phys. Lett.* **7** 499 (1981)]
77. Shlager K L, Smith G S, Maloney J G *IEEE Trans. Electromagn. Compat.* **EC-38** 413 (1996)
78. Lewis I A D, Wells F M *Millimicrosecond Pulse Techniques* (London: Pergamon Press, 1954) [Translated into Russian (Moscow: IL, 1956)]
79. Theodorou E A et al. *IEE Proc. H: Microwaves, Opt. Antennas* **128H** (3) 124 (1981)
80. Gubanov V P et al. *Pis'ma Zh. Tekh. Fiz.* **20** (14) 89 (1994) [*Tech. Phys. Lett.* **20** 604 (1994)]
81. Baum C E, Farr E G, in *Ultra-Wideband, Short-Pulse Electromagnetics* (Eds H L Bertoni, L Karin, L B Felsen) (New York: Plenum Press, 1993) p. 139
82. Giri D V et al. *IEEE Trans. Plasma Sci.* **PS-25** 318 (1997)
83. Koshelev V I et al. *Proc. SPIE* **3158** 209 (1997)
84. Agee F J et al. *IEEE Trans. Plasma Sci.* **PS-26** 860 (1998)
85. Skolnik M I (Ed.-in-Chief) *Radar Handbook* (New York: McGraw-Hill, 1970)
86. Shpak V G et al. *Izv. Vyssh. Uchebn. Zaved., Fiz.* **39** (12) 119 (1996)